



Contents lists available at ScienceDirect

International Journal for Parasitology: Drugs and Drug Resistance

journal homepage: www.elsevier.com/locate/ijpddr

Activity of (1-benzyl-4-triazolyl)-indole-2-carboxamides against *Toxoplasma gondii* and *Cryptosporidium parvum*

Shahbaz M. Khan^a, Anolan Garcia Hernandez^b, Idrees Mehraj Allaie^a, Gregory M. Grooms^b, Kun Li^{a,d}, William H. Witola^{a,**}, Jozef Stec^{b,c,*}

^a Department of Pathobiology, College of Veterinary Medicine, University of Illinois at Urbana-Champaign, 2001 S. Lincoln Avenue, Urbana, IL, 61802, USA

^b Chicago State University, College of Pharmacy, Department of Pharmaceutical Sciences, 9501 S. King Drive, Chicago, IL, 60628, USA

^c Marshall B. Ketchum University, College of Pharmacy, Department of Pharmaceutical Sciences, 2575 Yorba Linda Blvd., Fullerton, CA, 82831, USA

^d Institute of Traditional Chinese Veterinary Medicine, MOE Joint International Research Laboratory of Animal Health and Food Safety, College of Veterinary Medicine, Nanjing Agricultural University, Nanjing, 210095, PR China

ARTICLE INFO

Keywords:

Toxoplasma gondii

Cryptosporidium parvum

Antiprotozoal agents

Drug discovery

(1-Benzyl-4-triazolyl)-indole-2-carboxamides

(1-adamantyl)-4-phenyl-triazoles

ABSTRACT

Parasitic diseases such as toxoplasmosis and cryptosporidiosis remain serious global health challenges, not only to humans but also to domestic animals and wildlife. With only limited treatment options available, *Toxoplasma gondii* and *Cryptosporidium parvum* (the causative agents of toxoplasmosis and cryptosporidiosis, respectively) constitute a substantial health threat especially to young children and immunocompromised individuals. Herein, we report the synthesis and biological evaluation of a series of novel (1-benzyl-4-triazolyl)-indole-2-carboxamides and related compounds that show efficacy against *T. gondii* and *C. parvum*. Closely related analogs **7c** (JS-2-30) and **7e** (JS-2-44) showed low micromolar activity with IC₅₀ indices ranging between 2.95 μM and 7.63 μM against both *T. gondii* and *C. parvum*, whereas the compound representing (1-adamantyl)-4-phenyl-triazole, **11b** (JS-2-41), showed very good activity with an IC₅₀ of 1.94 μM, and good selectivity against *T. gondii* *in vitro*. Importantly, compounds JS-2-41 and JS-2-44 showed appreciable *in vivo* efficacy in decreasing the number of *T. gondii* cysts in the brains of Brown Norway rats. Together, these results indicate that (1-benzyl-4-triazolyl)-indole-2-carboxamides and (1-adamantyl)-4-phenyl-triazoles are potential hits for medicinal chemistry explorations in search for novel antiparasitic agents for effective treatment of cryptosporidiosis and toxoplasmosis.

1. Introduction

Toxoplasmosis and cryptosporidiosis represent zoonotic diseases (also known as zoonoses) that spread between animals and people (Centers for Disease Control and Prevention (CDC), 2022a). Although not as lethal as malaria, toxoplasmosis represents one of the world's most prevalent parasitic diseases infecting most genera of warm-blooded animals (more than 30 species of birds and 300 species of mammals) (Flegr et al., 2014). In the US alone, more than 40 million individuals are infected with *Toxoplasma gondii* (*T. gondii*), and the infection is considered to be a leading cause of death attributed to a foodborne illness (Centers for Disease Control and Prevention (CDC), 2022b). It is estimated that 30–50% of the world's population harbor the

parasite, which makes *T. gondii* the most prevalent parasite-caused infection in humans (Flegr et al., 2014). In immunocompetent individuals, *T. gondii* infection is usually mild because the host immune system prevents the development of illness. However, the infection is of concern in pregnant women, congenitally infected neonates, immunocompromised patients (e.g. HIV positive individuals), and in transplant or cancer patients treated with immunosuppressive agents (Flegr et al., 2014). Serious complications of toxoplasmosis are associated with differentiation of *T. gondii* parasites into bradyzoites that are clustered within cysts (pseudocysts) and sequestered in muscle and brain tissues of the host, representing the persistent stage of the infection. Reactivation and differentiation of the bradyzoites back to the replicative stage (tachyzoites) leads to damage of the infected tissues (Jeffers et al.,

* Corresponding author. Marshall B. Ketchum University, College of Pharmacy, Department of Pharmaceutical Sciences, 2575 Yorba Linda Blvd., Fullerton, CA, 82831, USA.

** Corresponding author. Department of Pathobiology, College of Veterinary Medicine, University of Illinois at Urbana-Champaign, 2001 S. Lincoln Avenue, Urbana, IL, 61802, USA.

E-mail addresses: whwit35@illinois.edu (W.H. Witola), jstec@ketchum.edu (J. Stec).

<https://doi.org/10.1016/j.ijpddr.2022.04.001>

Received 18 February 2022; Received in revised form 30 March 2022; Accepted 5 April 2022

Available online 16 April 2022

2211-3207/© 2022 Published by Elsevier Ltd on behalf of Australian Society for Parasitology. This is an open access article under the CC BY-NC-ND license (<http://creativecommons.org/licenses/by-nc-nd/4.0/>).

2018).

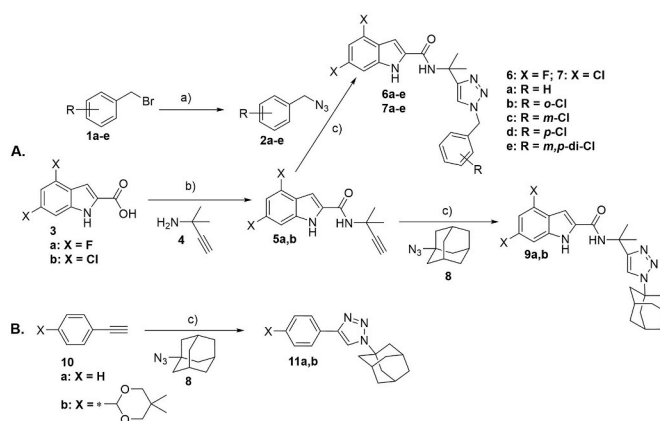
Similar to toxoplasmosis, cryptosporidiosis is self-limiting in immunocompetent persons. However, the infection poses a significant health threat to immunocompromised individuals and is responsible for an estimated 10–15% cases of severe diarrheal illness mostly in malnourished children below the age of five years (Gerace et al., 2019). The causative agent of this infection, *Cryptosporidium parvum* (*C. parvum*), is ranked as one of the leading cause of waterborne disease among humans in the United States (Centers for Disease Control and Prevention (CDC), 2022c). *C. parvum* is also a common veterinary pathogen responsible for a diarrheal syndrome in neonatal bovine calves resulting in substantial economic losses for farmers across the globe (Gerace et al., 2019).

Drug repurposing/repositioning is one of the major approaches to the discovery of new therapeutic applications for known medicines (*aka new use for an old drug*) (Austin et al., 2021; Kale et al., 2022). Practically all the medications used currently to combat toxoplasmosis were developed and initially approved for the treatment of different diseases (Andrews et al., 2014). Pyrimethamine was first approved for the treatment of malaria whereas sulfadiazine is a sulfonamide-based antibacterial agent. Used in combination, these two medications are now the treatment of choice for toxoplasmosis (Andrews et al., 2014). Combination of pyrimethamine with the lincosamide antibiotic - clindamycin is an alternative regimen recommended for the treatment and long-term maintenance therapy of *T. gondii* encephalitis and pneumonitis (Andrews et al., 2014). Another combination drug, co-trimoxazole (i.e. trimethoprim and sulfamethoxazole, TMP-SMX) was initially approved as antibacterial agent for the treatment of several infections such as urinary tract, middle ear, bronchitis, traveler's diarrhea, and shigellosis. However, it also found an off-label use in the prophylaxis, treatment of, or as chronic maintenance therapy for *T. gondii* encephalitis in adolescent and adult HIV-infected patients (Centers for Disease Control and Prevention (CDC), 2022d). Atovaquone, an antimalarial agent, has been repurposed for the treatment of *T. gondii* infections, whereas the macrolide antibiotic spiramycin is used in certain countries for the treatment of congenital toxoplasmosis (Andrews et al., 2014). More recently, another antibiotic from the macrolide class, azithromycin, was shown to control *T. gondii* infections (Castro-Filice et al., 2014). In a similar fashion, nitazoxanide, the only FDA-approved anti-*Cryptosporidium* drug in humans, was initially discovered as a veterinary anthelmintic agent and subsequent studies revealed its broad antiparasitic activity (Bolia 2020). Furthermore, a panel of diverse marketed agents approved for various conditions was screened against *C. parvum* and some of those medications were identified to have substantial activity against the parasite (Fritzler and Zhu, 2012; Guo et al., 2018). Accordingly, one of the current approaches utilized in anti-toxoplasmosis drug discovery is based on repurposing known hits, leads, or even entire libraries of compounds from other drug discovery campaigns. Examples of such

repurposed lead compounds include the spiroindolone NITD609 (Rottmann et al., 2010; Zhou et al., 2014), piperazine acetamide (Boyom et al., 2014; Van Voorhis et al., 2016), as well as benzoxaboroles AN3661 (Palencia et al., 2017; Sonoiki et al., 2017) and AN13762 (Zhang et al., 2017; Bellini et al., 2020) (Fig. 1A); all of which were initially discovered as antiparasitodal agents and subsequently were shown to be also active against *T. gondii*.

Herein, we report structure modification of the highly active antimycobacterial lead compound JS-2-02 (Stec et al., 2016) that targets the mycobacterial MmpL3 transporter and shows high efficacy *in vitro* and *in vivo* (Lun et al., 2013, 2019). Rationale to prepare and test the triazole analogs of JS-2-02 against *T. gondii* and *C. parvum* stems from the fact that the small molecule SQ109, which was originally reported as an effective inhibitor of mycobacterial MmpL3 (Tahlan et al., 2012) and is currently being investigated in clinical trials for tuberculosis, has shown potent efficacy against protozoan parasites including *T. gondii* (Li et al., 2015; Baek et al., 2022). While bona fide MmpL3 transporter has not been identified in *T. gondii* or *C. parvum*, MmpL3-like proteins have been proposed to be present in many protozoa among other living organisms (Malwal et al., 2021; Malwal and Oldfield, 2022).

Medicinal chemistry structure exploration of the original indole-2-carboxamide scaffold resulted in the synthesis of a series of (1-benzyl-4-triazolyl)-indole-2-carboxamides and related compounds, which displayed *in vitro* antiparasitodal activity against *T. gondii* and *C. parvum*



Scheme 1. (A) Synthesis of (1-benzyl-4-triazolyl)-indole-2-carboxamides (6/7a-e) and their 1-adamantyl analogs (9a,b). (B) Synthesis of (1-adamantyl)-4-phenyl-triazoles (11a,b). Reagents and conditions: a) NaN_3 (2.0 equiv), dry DMF, 100 °C, 18 h, 86–100%. b) EDC-HCl (1.0 equiv), HOBt (1.0 equiv), Et_3N (1.5 equiv), CH_2Cl_2 , RT, 12–16 h, 58–68%. c) sodium ascorbate (0.1 equiv), $\text{CuSO}_4 \cdot 5\text{H}_2\text{O}$ (0.1 equiv), tBuOH/ H_2O (1:1), RT, 14–21 h, 18–89%.

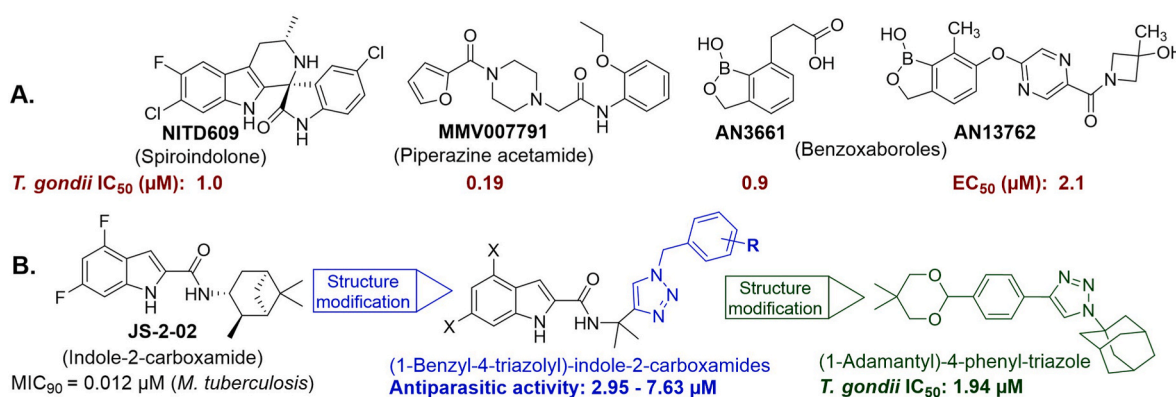


Fig. 1. (A) Examples of lead compounds initially discovered as antimalarial agents that have shown anti-*Toxoplasma* activity. (B) Modification of the antitubercular lead compound JS-2-02 into a new series of (1-benzyl-4-triazolyl)-indole-2-carboxamides with significant anti-*Toxoplasma gondii* and anti-*Cryptosporidium parvum* activity.

(Fig. 1B). Compounds **7e** (JS-2-44) and **11b** (JS-2-41) (Scheme 1) also showed significant activity *in vivo* in eliminating *T. gondii* cysts in the brains of male Brown Norway rats.

2. Materials and methods

2.1. Chemistry

2.1.1. General information

All reagents and solvents were purchased from Sigma-Aldrich and Fisher Scientific. Anhydrous dimethylformamide (DMF) was purchased from Sigma-Aldrich whereas anhydrous dichloromethane (DCM) was obtained by distillation over calcium hydride. ^1H NMR and ^{13}C NMR spectra were recorded on JEOL spectrometer at 400 and 100 MHz, respectively. NMR spectra were reprocessed by ACD/NMR Processor Academic Edition version 12.01. Standard abbreviations indicating multiplicity were used as follows: s = singlet, d = doublet, dd = doublet of doublets, t = triplet, q = quadruplet, m = multiplet, and br = broad. HR-MS experiments were performed on Agilent 6224 ToF-MS instrument. TLC was performed on Merck 60 F254 silica gel plates. Flash chromatography was performed using a Biotage - Isolera™ system with pre-packed silica columns (Biotage FLSH SNAP CRT SI 10, 25, or 50 g). All tested compounds were $\geq 95\%$ pure as determined by ^1H NMR and analytical HPLC: Shimadzu LC-2010 all-in-one system equipped with auto-injector and UV/Vis detector (variable wavelength). The system was controlled by LabSolutions™ (Shimadzu) running under Windows 7. The used method: flow rate = 1.4 mL/min; gradient elution over 20 min, from 30% MeOH/H₂O to 100% MeOH with 0.05% TFA with Phenomenex Synergi 4 μm Hydro-RP 80A column, 150 mm.

2.1.2. Analytical data of the synthesized compounds

(5a. JS-2-15) 4,6-Difluoro-N-(2-methylbut-3-yn-2-yl)-1H-indole-2-carboxamide: Pale yellow solid, 5.33 g (68%).

^1H NMR (400 MHz, DMSO-*d*₆) δ ppm 11.93 (s, 1H), 8.29 (d, 1H), 7.30 (s, 1H), 6.98 (dd, *J* = 9.6, 1.4 Hz, 1H), 6.83 (td, *J* = 10.4, 2.1 Hz, 1H), 3.11 (s, 1H), 1.85 (s, 6H).

^{13}C NMR (100 MHz, DMSO-*d*₆) δ ppm 160.2 (C), 159.8 (C, *d*, *J* = 238.7, 12.5 Hz), 156.3 (C, *d*, *J* = 248.7, 15.8 Hz), 138.1 (C, dd, *J* = 15.3, 13.4 Hz), 133.3 (C, *d*, *J* = 3.8 Hz), 113.6 (C, *d*, *J* = 21.1 Hz), 99.5 (CH), 95.7 (C, *d*, *J* = 29.9, 24.0 Hz), 95.1 (C, *d*, *J* = 25.9, 4.8 Hz), 88.3 (C), 71.6 (CH), 47.2 (C), 29.6 (2CH₃).

HRMS (TOF): *m/z* [M]⁺ calculated for C₁₄H₁₂F₂N₂O: 262.0918; found: 262.0924.

(5b. JS-2-22) 4,6-Dichloro-N-(2-methylbut-3-yn-2-yl)-1H-indole-2-carboxamide: Pale yellow solid, 1.50 g (58%).

^1H NMR (400 MHz, DMSO-*d*₆) δ ppm 12.02 (s, 1H), 8.44 (s, 1H), 7.37 (br s, 1H), 7.33 (br s, 1H), 7.18 (t, *J* = 1.4 Hz, 1H), 3.12 (d, *J* = 1.4 Hz, 1H), 1.59 (s, 6H).

^{13}C NMR (100 MHz, DMSO-*d*₆) δ ppm 160.1 (C), 137.3 (C), 134.0 (C), 128.3 (C), 126.9 (C), 125.3 (C), 119.9 (CH), 111.6 (CH), 101.9 (CH), 88.2 (C), 71.7 (CH), 47.3 (C), 29.6 (2CH₃).

HRMS (TOF): *m/z* [M]⁺ calculated for C₁₄H₁₂Cl₂N₂O: 294.0327; found: 294.0331.

(6a. JS-2-18) N-(2-(1-Benzyl-1H-1,2,3-triazol-4-yl)propan-2-yl)-4,6-difluoro-1H-indole-2-carboxamide: Off-white solid, 201 mg (51%).

^1H NMR (400 MHz, DMSO-*d*₆) δ ppm 11.83 (s, 1H), 8.63 (s, 1H), 7.96 (s, 1H), 7.35–7.25 (m, 6H), 6.95 (dd, *J* = 9.4, 1.6 Hz, 1H), 6.83 (td, *J* = 10.4, 2.1 Hz, 1H), 5.49 (s, 2H), 1.67 (br s, 6H).

^{13}C NMR (100 MHz, DMSO-*d*₆) δ ppm 160.2 (C), 159.7 (C, dd, *J* = 238.7, 11.5 Hz), 156.2 (C, dd, *J* = 248.3, 15.3 Hz), 153.6 (C), 138.0 (C, t, *J* = 14.4 Hz), 136.8 (C), 133.7 (C, *d*, *J* = 3.8 Hz), 129.2 (2CH), 128.5 (CH), 128.4 (2CH), 122.1 (CH), 113.6 (C, *d*, *J* = 22.1 Hz), 99.4 (CH), 95.7 (CH, dd, *J* = 29.7, 24.6 Hz), 95.1 (CH, dd, *J* = 25.9, 3.8 Hz), 53.1 (CH₂), 51.6 (C), 28.9 (2CH₃).

HRMS (TOF): *m/z* [M]⁺ calculated for C₂₁H₁₉F₂N₅O: 395.1558;

found: 395.1561.

(6b. JS-2-25) N-(2-(1-(2-Chlorobenzyl)-1H-1,2,3-triazol-4-yl)propan-2-yl)-4,6-difluoro-1H-indole-2-carboxamide: Off-white solid, 235 mg (55%).

^1H NMR (400 MHz, DMSO-*d*₆) δ ppm 11.83 (s, 1H), 8.38 (s, 1H), 7.96 (s, 1H), 7.47 (dd, *J* = 7.8, 1.8 Hz, 1H), 7.36–7.29 (m, 3H), 7.08 (dd, *J* = 7.6, 2.1 Hz, 1H), 6.95 (dd, *J* = 9.2, 1.4 Hz, 1H), 6.83 (dd, *J* = 10.4, 2.1 Hz, 1H), 5.61 (s, 2H), 1.69 (s, 6H).

^{13}C NMR (100 MHz, DMSO-*d*₆) δ ppm 160.2 (C), 159.7 (C, dd, *J* = 238.2, 12.0 Hz), 156.2 (C, dd, *J* = 248.2, 15.3 Hz), 153.5 (C), 138.0 (C, dd, *J* = 15.3, 13.4 Hz), 134.1 (C), 133.6 (C, *d*, *J* = 2.9 Hz), 132.9 (C), 130.6 (CH), 130.5 (C), 130.1 (CH), 128.2 (CH), 122.5 (CH), 113.6 (C, *d*, *J* = 22.1 Hz), 99.4 (CH), 95.7 (CH, dd, *J* = 29.7, 24.0 Hz), 95.1 (CH, dd, *J* = 25.9, 3.8 Hz), 51.6 (C), 50.8 (CH₂), 28.8 (2CH₃).

HRMS (TOF): *m/z* [M]⁺ calculated for C₂₁H₁₈ClF₂N₅O: 429.1168; found: 429.1166.

(6c. JS-2-26) N-(2-(1-(3-Chlorobenzyl)-1H-1,2,3-triazol-4-yl)propan-2-yl)-4,6-difluoro-1H-indole-2-carboxamide: Off-white solid, 230 mg (54%).

^1H NMR (400 MHz, DMSO-*d*₆) δ ppm 11.82 (s, 1H), 8.37 (s, 1H), 8.01 (s, 1H), 7.36–7.34 (m, 4H), 7.21 (m, 1H), 6.95 (dd, *J* = 9.4, 1.6 Hz, 1H), 6.83 (td, *J* = 10.3, 1.8 Hz, 1H), 5.51 (s, 2H), 1.68 (s, 6H).

^{13}C NMR (100 MHz, DMSO-*d*₆) δ ppm 160.2 (C), 159.7 (C, dd, *J* = 238.2, 12.0 Hz), 156.2 (C, dd, *J* = 248.2, 15.3 Hz), 153.7 (C), 139.2 (C), 138.0 (C, dd, *J* = 28.8, 13.4 Hz), 133.7 (C), 133.6 (C, *d*, *J* = 3.8 Hz), 131.2 (CH), 128.6 (CH), 128.4 (CH), 127.1 (CH), 122.2 (CH), 113.6 (C, *d*, *J* = 22.1 Hz), 99.5 (CH), 95.7 (CH, dd, *J* = 29.2, 23.5 Hz), 95.1 (CH, dd, *J* = 26.4, 4.3), 52.3 (CH₂), 51.6 (C), 28.9 (2CH₃).

HRMS (TOF): *m/z* [M]⁺ calculated for C₂₁H₁₈ClF₂N₅O: 429.1168; found: 429.1165.

(6d. JS-2-32) N-(2-(1-(4-Chlorobenzyl)-1H-1,2,3-triazol-4-yl)propan-2-yl)-4,6-difluoro-1H-indole-2-carboxamide: White solid, 176 mg (58%).

^1H NMR (400 MHz, DMSO-*d*₆) δ ppm 11.82 (s, 1H), 8.37 (s, 1H), 7.97 (s, 1H), 7.40 (d, *J* = 8.2 Hz, 2H), 7.33 (d, *J* = 1.8 Hz, 1H), 7.29 (d, *J* = 8.2 Hz, 2H), 6.95 (dd, *J* = 9.4, 1.6 Hz, 1H), 6.83 (td, *J* = 10.4, 2.1 Hz, 1H), 5.50 (s, 2H), 1.67 (s, 6H).

^{13}C NMR (100 MHz, DMSO-*d*₆) δ ppm 160.2 (C), 159.7 (C, dd, *J* = 238.2, 12.0 Hz), 156.3 (C, dd, *J* = 248.7, 15.8 Hz), 153.6 (C), 138.0 (C, t, *J* = 13.9 Hz), 135.8 (C), 133.6 (C, *d*, *J* = 2.9 Hz), 133.3 (C), 130.4 (2CH), 129.2 (2CH), 122.1 (CH), 113.6 (C, *d*, *J* = 22.1 Hz), 99.4 (CH), 95.7 (CH, dd, *J* = 29.7, 24.0 Hz), 95.1 (CH, dd, *J* = 25.4, 3.4 Hz), 52.3 (CH₂), 51.6 (C), 28.8 (2CH₃).

HRMS (TOF): *m/z* [M]⁺ calculated for C₂₁H₁₈ClF₂N₅O: 429.1168; found: 429.1164.

(6e. JS-2-43) N-(2-(1-(3,4-Dichlorobenzyl)-1H-1,2,3-triazol-4-yl)propan-2-yl)-4,6-difluoro-1H-indole-2-carboxamide: Off-white solid, 184 mg (79%).

^1H NMR (400 MHz, DMSO-*d*₆) δ ppm 11.81 (s, 1H), 8.37 (s, 1H), 8.02 (s, 1H), 7.61 (d, *J* = 8.2 Hz, 1H), 7.58 (d, *J* = 1.8 Hz, 1H), 7.34 (dd, *J* = 2.3, 0.9 Hz, 1H), 7.24 (dd, *J* = 8.2, 1.8 Hz, 1H), 6.95 (dd, *J* = 9.6, 1.4 Hz, 1H), 6.83 (dt, *J* = 10.4, 2.1 Hz, 1H), 5.52 (s, 2H), 1.68 (s, 6H).

^{13}C NMR (100 MHz, DMSO-*d*₆) δ ppm 160.2 (C), 159.7 (C, dd, *J* = 238.2, 12.0 Hz), 156.2 (C, dd, *J* = 248.2, 15.3 Hz), 153.7 (C), 138.0 (C, t, *J* = 14.4 Hz), 137.8 (C), 133.6 (C, *d*, *J* = 2.9 Hz), 131.7 (C), 131.5 (CH), 131.3 (C), 130.6 (CH), 128.9 (CH), 122.3 (CH), 113.6 (C, *d*, *J* = 22.1 Hz), 99.5 (CH), 95.7 (CH, dd, *J* = 29.7, 23.0 Hz), 95.1 (CH, dd, *J* = 25.9, 3.8 Hz), 51.7 (CH₂), 51.6 (C), 28.8 (2CH₃).

HRMS (TOF): *m/z* [M]⁺ calculated for C₂₁H₁₇Cl₂F₂N₅O: 463.0778; found: 463.0777.

(7a. JS-2-27) N-(2-(1-Benzyl-1H-1,2,3-triazol-4-yl)propan-2-yl)-4,6-dichloro-1H-indole-2-carboxamide: Off-white solid, 190 mg (89%).

^1H NMR (400 MHz, DMSO-*d*₆) δ ppm 11.91 (d, *J* = 1.8 Hz, 1H), 8.53 (s, 1H), 7.97 (s, 1H), 7.38 (dd, *J* = 2.3, 0.9 Hz, 1H), 7.34–7.25 (m, 6H), 7.18 (d, *J* = 1.4 Hz, 1H), 5.49 (s, 2H), 1.68 (s, 6H).

^{13}C NMR (100 MHz, DMSO- d_6) δ ppm 160.2 (C), 153.5 (C), 137.2 (C), 136.8 (C), 134.4 (C), 129.2 (2CH), 128.5 (CH), 128.4 (2CH), 128.1 (C), 126.9 (C), 125.3 (C), 122.1 (CH), 119.9 (CH), 111.5 (CH), 101.8 (CH), 53.1 (CH₂), 51.7 (C), 28.9 (2CH₃).

HRMS (TOF): m/z [M]⁺ calculated for C₂₁H₁₉Cl₂N₅O: 427.0967; found: 427.0966.

(7b. JS-2-28) 4,6-Dichloro-N-(2-(1-(2-chlorobenzyl)-1H-1,2,3-triazol-4-yl)propan-2-yl)-1H-indole-2-carboxamide: Pale brown solid, 156 mg (67%).

^1H NMR (400 MHz, DMSO- d_6) δ ppm 11.91 (d, $J = 1.8$ Hz, 1H), 8.54 (s, 1H), 7.97 (s, 1H), 7.47 (dd, $J = 7.6$ Hz, 1H), 7.38–7.28 (m, 4H), 7.17 (d, $J = 1.8$ Hz, 1H), 7.08 (dd, $J = 7.3, 2.3$ Hz, 1H), 5.61 (s, 2H), 1.69 (s, 6H).

^{13}C NMR (100 MHz, DMSO- d_6) δ ppm 160.2 (C), 153.5 (C), 137.2 (C), 134.3 (C), 134.1 (C), 132.9 (C), 130.6 (C), 130.5 (CH), 130.1 (CH), 128.2 (CH), 128.1 (C), 126.9 (C), 125.3 (C), 122.5 (CH), 119.9 (CH), 111.5 (CH), 101.8 (CH), 51.7 (C), 50.8 (CH₂), 28.8 (2CH₃).

HRMS (TOF): m/z [M]⁺ calculated for C₂₁H₁₈Cl₃N₅O: 461.0577; found: 461.0571.

(7c. JS-2-30) 4,6-Dichloro-N-(2-(1-(3-chlorobenzyl)-1H-1,2,3-triazol-4-yl)propan-2-yl)-1H-indole-2-carboxamide: Pale yellow solid, 177 mg (76%).

^1H NMR (400 MHz, DMSO- d_6) δ ppm 11.90 (d, $J = 1.4$ Hz, 1H), 8.53 (s, 1H), 8.02 (s, 1H), 7.38 (d, $J = 1.4$ Hz, 1H), 7.36–7.35 (m, $J = 4.6, 0.9$ Hz, 4H), 7.21 (m, 1H), 7.17 (d, $J = 1.8$ Hz, 1H), 5.51 (s, 2H), 1.68 (br s, 6H).

^{13}C NMR (100 MHz, DMSO- d_6) δ ppm 160.2 (C), 153.6 (C), 139.2 (C), 137.2 (C), 134.3 (C), 133.7 (C), 131.2 (CH), 128.6 (CH), 128.4 (CH), 128.1 (C), 127.1 (CH), 126.9 (C), 125.3 (C), 122.2 (CH), 119.9 (CH), 111.5 (CH), 101.9 (CH), 52.3 (CH₂), 51.7 (C), 28.8 (2CH₃).

HRMS (TOF): m/z [M]⁺ calculated for C₂₁H₁₈Cl₃N₅O: 461.0577; found: 461.0575.

(7d. JS-2-33) 4,6-Dichloro-N-(2-(1-(4-chlorobenzyl)-1H-1,2,3-triazol-4-yl)propan-2-yl)-1H-indole-2-carboxamide: Off-white solid, 180 mg (65%).

^1H NMR (400 MHz, DMSO- d_6) δ ppm 11.89 (d, $J = 1.8$ Hz, 1H), 8.53 (s, 1H), 7.98 (s, 1H), 7.41–7.38 (m, 3H), 7.34 (dd, $J = 1.8, 0.9$ Hz, 1H), 7.29 (d, $J = 8.7, 1.6$ Hz, 2H), 7.17 (d, $J = 1.4$ Hz, 1H), 5.50 (s, 2H), 1.68 (s, 6H).

^{13}C NMR (100 MHz, DMSO- d_6) δ ppm 160.2 (C), 153.6 (C), 137.2 (C), 135.8 (C), 134.3 (C), 133.3 (C), 130.4 (2CH), 129.2 (2CH), 128.1 (C), 126.9 (C), 125.3 (C), 122.1 (CH), 119.9 (CH), 111.5 (CH), 101.8 (CH), 52.3 (CH₂), 51.7 (C), 28.8 (2CH₃).

HRMS (TOF): m/z [M]⁺ calculated for C₂₁H₁₈Cl₃N₅O: 461.0577; found: 461.0576.

(7e. JS-2-44) 4,6-Dichloro-N-(2-(1-(3,4-dichlorobenzyl)-1H-1,2,3-triazol-4-yl)propan-2-yl)-1H-indole-2-carboxamide: Off-white solid, 127 mg (51%).

^1H NMR (400 MHz, DMSO- d_6) δ ppm 11.89 (d, $J = 1.8$ Hz, 1H), 8.53 (s, 1H), 8.03 (s, 1H), 7.61 (d, $J = 8.2$ Hz, 1H), 7.58 (d, $J = 2.3$ Hz, 1H), 7.38 (dd, $J = 2.3, 0.9$ Hz, 1H), 7.34 (dd, $J = 1.8, 0.9$ Hz, 1H), 7.24 (dd, $J = 8.2, 2.3$ Hz, 1H), 7.17 (d, $J = 1.4$ Hz, 1H), 5.52 (s, 2H), 1.68 (br s, 6H).

^{13}C NMR (100 MHz, DMSO- d_6) δ ppm 160.2 (C), 153.7 (C), 137.8 (C), 137.2 (C), 134.3 (C), 131.7 (C), 131.5 (C), 131.3 (C), 130.6 (CH), 128.9 (CH), 128.1 (C), 126.9 (C), 125.3 (C), 122.3 (CH), 119.9 (CH), 111.5 (CH), 101.9 (CH), 51.7 (CH₂), 51.7 (overlap C), 28.8 (2CH₃).

HRMS (TOF): m/z [M]⁺ calculated for C₂₁H₁₇Cl₄N₅O: 495.0187; found: 495.0159.

(9a. JS-2-19) N-(2-(1-(Adamantan-1-yl)-1H-1,2,3-triazol-4-yl)propan-2-yl)-4,6-difluoro-1H-indole-2-carboxamide: White solid, 173 mg (36%).

^1H NMR (400 MHz, DMSO- d_6) δ ppm 11.85 (s, 1H), 8.31 (s, 1H), 7.95 (s, 1H), 7.33 (d, $J = 1.4$ Hz, 1H), 6.94 (dd, $J = 9.4, 1.6$ Hz, 1H), 6.82 (td, $J = 10.4, 2.1$ Hz, 1H), 2.11 (br s, 9H), 1.69–1.68 (m, 12H).

^{13}C NMR (100 MHz, DMSO- d_6) δ ppm 160.2 (C), 159.7 (C, dd, $J = 238.7, 12.5$ Hz), 156.2 (C, dd, $J = 248.2, 15.3$ Hz), 152.7 (C), 138.0 (C,

apparent dd, $J = 15.3, 13.4$ Hz), 133.8 (C, d, $J = 2.9$ Hz), 118.3 (CH), 113.6 (C, d, $J = 22.1$ Hz), 99.4 (CH), 95.6 (CH, dd, $J = 29.7, 24.0$ Hz), 95.0 (CH, dd, $J = 25.9, 4.8$ Hz), 59.1 (C), 51.7 (C), 42.8 (3CH₂), 35.8 (3CH₂), 29.4 (2CH₃), 28.8 (3CH).

HRMS (TOF): m/z [M]⁺ calculated for C₂₄H₂₇F₂N₅O: 439.2184; found: 439.2188.

(9b. JS-2-31) N-(2-(1-(Adamantan-1-yl)-1H-1,2,3-triazol-4-yl)propan-2-yl)-4,6-dichloro-1H-indole-2-carboxamide: Pale brown solid, 74 mg (31%).

^1H NMR (400 MHz, DMSO- d_6) δ ppm 11.93 (d, $J = 1.4$ Hz, 1H), 8.48 (s, 1H), 7.96 (s, 1H), 7.38 (d, $J = 1.4$ Hz, 1H), 7.34 (br s, 1H), 7.17 (d, $J = 1.8$ Hz, 1H), 2.11 (br s, 9H), 1.69–1.68 (m, 12H).

^{13}C NMR (100 MHz, DMSO- d_6) δ ppm 160.1 (C), 152.6 (C), 137.1 (C), 134.5 (C), 128.1 (C), 126.9 (C), 125.3 (C), 119.8 (CH), 118.3 (CH), 111.5 (CH), 101.8 (CH), 59.1 (C), 51.8 (C), 42.8 (3CH₂), 35.8 (3CH₂), 29.4 (2CH₃), 28.8 (3CH).

HRMS (TOF): m/z [M]⁺ calculated for C₂₄H₂₇Cl₂N₅O: 471.1593; found: 471.1590.

(11a. JS-2-40) 1-(Adamantan-1-yl)-4-phenyl-1H-1,2,3-triazole: Pale yellow solid, 66 mg (24%).

^1H NMR (400 MHz, DMSO- d_6) δ ppm 8.65 (s, 1H), 7.83–7.81 (dd, $J = 6.9, 1.4$ Hz, 2H), 7.39 (t, $J = 7.8$ Hz, 2H), 7.27 (tt, $J = 7.3, 1.4$ Hz, 1H), 2.18 (br s, 9H), 1.71 (br s, 6H).

^{13}C NMR (100 MHz, DMSO- d_6) δ ppm 146.2 (C), 131.6 (C), 129.4 (2CH), 128.2 (CH), 125.6 (2CH), 118.8 (CH), 59.6 (C), 42.8 (3CH₂), 35.9 (3CH₂), 29.4 (3CH).

HRMS (TOF): m/z [M]⁺ calculated for C₁₈H₂₁N₃: 279.1735; found: 279.1736.

(11b. JS-2-41) 1-(Adamantan-1-yl)-4-(4-(5,5-dimethyl-1,3-dioxan-2-yl)phenyl)-1H-1,2,3-triazole: Pale yellow solid, 70 mg (18%).

^1H NMR (400 MHz, DMSO- d_6) δ ppm 8.68 (s, 1H), 7.82 (d, $J = 8.24$ Hz, 2H), 7.44 (d, $J = 8.24$ Hz, 2H), 5.38 (s, 1H), 3.62 (m, 4H), 2.18 (br s, 9H), 1.71 (br s, 6H), 1.15 (s, 3H), 0.71 (s, 3H).

^{13}C NMR (100 MHz, DMSO- d_6) δ ppm 145.9 (C), 138.5 (C), 131.9 (C), 127.2 (2CH), 125.2 (2CH), 119.0 (CH), 101.1 (CH), 77.0 (2CH₂), 59.6 (C), 42.8 (4CH₂), 35.9 (2CH₂), 30.4 (C), 29.4 (3CH), 23.3 (CH₃), 21.9 (CH₃).

HRMS (TOF): m/z [M]⁺ calculated for C₂₄H₃₁N₃O₂: 393.2416; found: 393.2415.

2.2. Biology

2.2.1. Parasites and host cells

The type I RH strain of *T. gondii*, stably expressing cytoplasmic yellow fluorescent protein (YFP) (Gubbels et al., 2003) and the luciferase-expressing type II ME49 strain of *T. gondii* (ME49ΔHPT::Luc) (Tobin and Knoll, 2012) were used in this study. Parasites were maintained in human foreskin fibroblast cells (HFF-1) (ATCC® SCRC-1041™) and cultured in Iscove's modified Dulbecco's medium (IMDM) supplemented with 10% heat-inactivated fetal bovine serum (FBS) (Gibco, USA), 1 × GlutaMAX™ supplement (Gibco, USA), and 1 × Antibiotic-Antimycotic (Gibco, USA) in a humidified incubator at 37 °C with 5% CO₂. *T. gondii* tachyzoites were harvested by passing the infected HFF cells through a 25-gauge needle two times and filtering the ruptured cell suspension through a sterile 5 μm syringe filter unit (Millex™; Millipore, USA) to remove the host cell debris and isolate the parasites. The extracted tachyzoites were counted using a hemocytometer and used immediately for infection assays.

The *C. parvum* AUCP-1 isolate used for the experiments described in this study was maintained and propagated in male Holstein calves. *C. parvum* oocysts were extracted and purified from freshly collected calf feces by sequential sieve filtration, Sheather's sugar flotation, and discontinuous sucrose density gradient centrifugation (Arrowood and Sterling, 1987; Current, 1990). Purified oocysts were washed and stored in phosphate-buffered saline (PBS) at 4 °C and used within 3 months to

ensure maximum viability. *C. parvum* sporozoites were excysted from oocysts following the method reported previously (Kuhlenschmidt et al., 2016). Briefly, 1×10^8 purified *C. parvum* oocysts were suspended in 500 μ l of PBS and treated with an equal volume of 40% commercial laundry bleach for 10 min at 4 °C, followed by four washes in PBS containing 1% bovine serum albumin. Oocysts were resuspended in Hanks balanced salt solution (HBSS), incubated for 60 min at 37 °C, and mixed with an equal volume of warm 1.5% sodium taurocholate in HBSS followed by further incubation for 60 min at 37 °C with occasional shaking. The excysted sporozoites were pelleted by centrifugation and resuspended in PBS. The sporozoites were separated from oocyst shells and unexcysted oocysts by passing the suspension through a sterile 5 μ m syringe filter unit (Millex™, Millipore, USA). Purified sporozoites were enumerated with a hemocytometer and used immediately for infection of cell monolayers.

2.2.2. In vitro compound cytotoxicity assays

A colorimetric assay using the cell proliferation reagent WST-1 (Roche, USA) was performed for the quantification of *in vitro* cytotoxicity of the test compounds. All compounds were initially tested for cytotoxicity at 20 μ M concentration in a human ileocecal colorectal adenocarcinoma cell line (HCT-8) (ATCC® CCL-244™), used for *in vitro* culture of *C. parvum*. Subsequently, non-toxic compounds that were found to have significant anti-*Cryptosporidium* and anti-*Toxoplasma* effects at 11 μ M were used at increasing concentrations (ranging from 0 to 400 μ M) to determine their half maximal cytotoxic concentrations (IC₅₀) in uninfected HCT-8 and HFF cells, respectively. Briefly, 5×10^4 HCT-8 cells were seeded per well in 96-well plates and grown overnight in 200 μ l of RPMI-1640 medium (without phenol red) (Gibco, USA) supplemented with 2.5 g/L of glucose, 1.5 g/L of sodium bicarbonate, 1 mM sodium pyruvate, 10% heat-inactivated FBS (Gibco, USA), and 1 \times Antibiotic-Antimycotic (Gibco, USA) at 37 °C with 5% CO₂ in a humidified incubator. HFF cells were seeded at a density of 1×10^4 cells per well in 96-well plates and allowed to grow in 200 μ l of IMDM (without phenol red) supplemented with 10% heat-inactivated FBS (Gibco, USA), 1 \times GlutaMAX™ supplement (Gibco, USA), and 1 \times Antibiotic-Antimycotic (Gibco, USA) at 37 °C with 5% CO₂. Once confluent, cells were treated with the test compounds reconstituted in molecular biology grade dimethyl sulfoxide (DMSO) (Sigma-Aldrich, USA) for 48 h. The volume of DMSO did not exceed 1% of the total culture volume in any of the wells to avoid DMSO toxicity to the cells. Control wells that received equivalent volumes of DMSO instead of the compound were also set up in parallel. Ten microliters of the WST-1 reagent were added to each well after 48 h of culture, and the plates were incubated for 1 h at 37 °C with 5% CO₂ under dark conditions. Following incubation, the plates were shaken thoroughly and 150 μ l of the medium from each well was transferred to a new clear flat-bottomed black 96-well plate (Corning, USA). The cleavage of the tetrazolium salt (WST-1) to formazan by metabolically active cells was quantified by reading the absorbance at a test wavelength of 440 nm and a reference wavelength of 690 nm using a multi-mode microplate reader (Spectra Max iD3; Molecular Devices, USA). The mean percent toxicity (MPT) of each compound was derived by dividing the difference in absorbance between the compound-treated cells and the DMSO-treated cells by the absorbance from the DMSO-treated cells and multiplying the product by 100:

$$\text{MPT} = [(\text{Mean OD}_{\text{DMSO treated}} - \text{Mean OD}_{\text{Compound treated}}) \div \text{Mean OD}_{\text{DMSO treated}}] \times 100$$

Compound cytotoxicity IC₅₀ values were determined by applying a non-linear regression analysis curve fit to the mean dose-response data of triplicate assays for each compound using GraphPad PRISM® v8.

2.2.3. In vitro testing of anti-Toxoplasma activity of compounds

All test compounds that showed no toxicity in HCT-8 cells at 20 μ M

were initially tested for *in vitro* *T. gondii* growth inhibition activity at 11 μ M concentration. Fresh supplemented IMDM medium was added to confluent HFF cell monolayers in 96-well plates and about 5×10^3 freshly extracted tachyzoites of *T. gondii* type I RH strain (constitutively expressing YFP) were added to each well. Immediately after infection, test compounds reconstituted in DMSO were added to one set of wells at a final concentration of 11 μ M. Atovaquone (Sigma-Aldrich, USA) reconstituted in DMSO was added to a separate set of wells as a positive control at a final concentration of 0.5 μ M (Araujo et al., 1991). Control infected cells were treated with volumes of DMSO equivalent to those used for the atovaquone and compound-treated cultures. The cells were placed in a humidified incubator at 37 °C with 5% CO₂, and parasite YFP fluorescence was analyzed by fluorescence microscopy after 48 h of incubation. Plates were imaged by using a 20 \times objective of an inverted fluorescence microscope. Fluorescence quantification of 9 representative images per well was done using the batch process function in ImageJ version v1.50 (NIH, USA) after setting a threshold for the detection of parasites. Control wells with uninfected monolayers were included for background subtraction. Assays were run in triplicate and repeated at least thrice.

2.2.4. In vitro testing of anti-Cryptosporidium activity of compounds

All compounds that showed no toxicity to HCT-8 cells in the primary cytotoxicity screening at 20 μ M were tested for inhibitory effect against the *in vitro* growth of *C. parvum* parasites at 11 μ M concentration. HCT-8 cells were seeded and grown to confluency in supplemented RPMI-1640 medium in 96-well plates. After replacing the old medium with fresh medium, plates were inoculated with 10^5 freshly excysted *C. parvum* sporozoites per well, immediately followed by the addition of test compounds (reconstituted in DMSO) to one set of wells at 11 μ M final concentration. Control infected cells were treated with volumes of DMSO equivalent to those used for the compound-treated cultures. Paromomycin reconstituted in distilled sterile water was added to a separate set of wells as a positive control at a final concentration of 400 μ M. The cultures were analyzed for parasite infectivity and proliferation by a direct immunofluorescence assay (Witola et al., 2017) after 72 h of culture. The medium was removed from the culture wells, and the cell monolayer was rinsed two times with PBS before fixation with pre-chilled methanol-acetic acid (9:1) for 5 min. The wells were rinsed with PBS to remove traces of fixative followed by two successive washes with buffer containing 0.1% Triton X-100, 0.35 M NaCl, and 0.13 M Tris-base, pH 7.6 to rehydrate and permeabilize the cells. Normal goat serum (5%) was used as a blocking solution, and the cell monolayer was stained with a fluorescein-labeled anti-*C. parvum* polyclonal antibody (Sporo-Glo™; Waterborne, Inc., USA) overnight at 4 °C. The stained cells were washed twice with PBS, followed by water, and then imaged with an inverted fluorescence microscope with a 20 \times objective. The fluorescence generated by intracellular *C. parvum* parasites was quantified from 9 representative images per well using the batch process function in Image J version 1.50 (NIH, USA) after setting a threshold for the detection of parasite stages. Control wells with uninfected monolayers were included for background subtraction. Experiments were performed in triplicates with at least three biological replicates.

2.2.5. Determination of anti-parasitic IC₅₀ values of compounds

To derive the half maximal inhibitory concentration (IC₅₀) values of the test compounds against the *T. gondii* type I RH strain, HFF cells were grown to confluency in 96-well plates and infected as described above, but instead of using a single concentration of test compounds, the cells were treated with increasing concentrations of test compounds. One set of HFF cells was treated with compounds immediately after infection with *T. gondii* tachyzoites, while the other set was treated with compounds 2 h after infection. Control infected cells received varying volumes of DMSO equivalent to the volumes used for the compound-treated cells. Atovaquone was used as a positive control and added at varying concentrations (0–1 μ M) to separate sets of wells immediately after

infection or 2 h p.i. The cells were analyzed by fluorescence microscopy after 48 h of incubation to measure parasite viability as described above. Samples were run in triplicate, and three independent assays were performed. IC₅₀ values were calculated using nonlinear regression analysis in GraphPad PRISM® v8.

IC₅₀ values of JS-2-41 and JS-2-44 against the *T. gondii* type II ME49 strain (constitutively expressing luciferase), were determined by infecting confluent HFF cells with approximately 1.5×10^4 freshly extracted tachyzoites and adding various concentrations of the compounds to the cultures immediately after infection. Control infected cells were treated immediately post infection with volumes of DMSO equivalent to those used in the compound-treated cultures while atovaquone added shortly p.i. at varying concentrations indicated above served as the positive control. The cultures were analyzed for parasite infectivity and proliferation after 48 h of incubation using the Luciferase Reporter Gene Assay high sensitivity kit (Roche, USA). Briefly, the medium was discarded from the wells, and the cells were lysed for 15 min at 37 °C and 5% CO₂ by adding 100 µl of Lysis buffer (Roche, USA) per well. The lysates were pipetted up and down several times and transferred to a white opaque-walled 96-well plate and 100 µl of the luciferase assay reagent (Roche, USA) added to each well. The luminescence generated by *T. gondii* luciferase activity was immediately measured using a multi-mode microplate reader (Spectra Max iD3; Molecular Devices, USA). Three independent assays were performed, and at least three technical replicates were included for each treatment. IC₅₀ values were calculated as described for *T. gondii* above.

Anti-*Cryptosporidium* IC₅₀ values of test compounds were derived by performing *in vitro* *C. parvum* infection assays in a similar manner as described above, with the exception that a range of increasing compound concentrations were used to treat infected HCT-8 cell cultures. One set of HCT-8 cells was treated with compounds immediately after infection with *C. parvum* sporozoites, while the other set was treated with compounds 2 h after infection. Control infected cells received varying volumes of DMSO equivalent to the ones used for the compound-treated cultures. Varying concentrations of paromomycin (0–500 µM) were added to separate sets of HCT-8 monolayers at the time of infection or 2 h p.i. as the positive control treatment. Cells were processed for immunofluorescence analysis after 72 h of incubation as described above. Three independent assays were performed, and samples were run in triplicate. IC₅₀ values were calculated using non-linear regression analysis of the mean dose-response curve data in GraphPad PRISM® v8.

2.2.6. Infection of rats with *Toxoplasma* and compound treatment

The protocol approved by the University of Illinois at Urbana-Champaign Institutional Animal Care and Use Committee was followed in performing experimental procedures involving rats. Fourteen male Brown Norway rats, aged 4 weeks, were obtained from Charles River, USA. After 7 days of acclimatization, the rats were allocated to four groups. This consisted of 3 treatment groups, each containing 3 rats, and one untreated group containing 5 rats. The rats in each group were inoculated intramuscularly with 5×10^4 freshly isolated *T. gondii* ME49 strain tachyzoites in 0.1 ml sterile PBS. After 5 weeks of infection, two rats in the “untreated” group were sacrificed and the brains excised and analyzed for the presence of *Toxoplasma* cysts. Briefly, intact rat brain was dissected out of the skull and placed in 5 ml sterile PBS and homogenized. Fifty microliters of the brain homogenate were placed on a glass slide and a cover slip applied. The entire slide field was examined using a light microscope 10 × objective, and the total number of *Toxoplasma* cysts present enumerated. The enumeration of cysts was performed on three independent slide preparations and the average number of cysts calculated. The number of cysts in the entire brain homogenate was derived by dividing the total brain homogenate volume (ml) by 0.05 ml and multiplying that by the average number of cysts enumerated on 3 slides preparations.

Upon confirmation of the presence *Toxoplasma* cysts in the rats’

brains, daily treatment of the rats in each treatment group commenced. Each rat in the JS-2-41, JS-2-44, and Atovaquone treatment, received a daily intraperitoneal injection dose of 3 mg/kg of JS-2-41, 4 mg/kg of JS-2-44, and 5 mg/kg of Atovaquone reconstituted in 0.2 ml 5% DMSO in PBS, respectively, for 2 weeks. The rats in the untreated group received an equivalent of 5% DMSO in PBS. After 2 weeks of daily treatment, the rats were sacrificed, the brains harvested, and the number of cysts enumerated as described above. Results were analyzed by one-way analysis of variance (ANOVA) with the Dunnett’s *post hoc* test for multiple comparisons between the treatments and the DMSO control. *P* values of 0.05 or less were considered significant.

3. Results

3.1. Chemistry

3.1.1. Synthesis of the test compounds

Various benzyl chlorides **1a-e** (Scheme 1A) were converted to the corresponding benzyl azides **2a-e** by following the previously reported method (Shi et al., 2008). 4,6-Difluoro- (**3a**) and 4,6-dichloroindole-2-carboxylic acids (**3b**) were reacted with 1,1-dimethylpropargylamine (**4**) according to the known synthetic protocol (Onajole et al., 2013) to give the corresponding amides (**5a,b**; JS-2-15,22). The intermediates **5a,b** were subsequently treated with various benzyl azides (**2a-e**) and 1-azidoadamantane (**8**), respectively, under standard conditions (Himo et al., 2005) to give (1-benzyl-4-triazolyl)- (**6/7a-e**; JS-2-18, 25, 26, 32, 43/27, 28, 30, 33 and 44) and (1-adamantyl-4-triazolyl)-indole-2-carboxamides (**9a,b**; JS-2-19 and 31), respectively (Scheme 1A). Reaction of ethynylbenzenes (**10a,b**) with 1-azidoadamantane (**8**) provided the corresponding compounds (**11a,b**; JS-2-40 and 41) (Scheme 1B). The isolated crude materials were purified by automated flash chromatography column to give pure final products in yields ranging from modest to very good (Table 1).

3.2. Biology

3.2.1. Cytotoxicity and anti-parasite evaluation of the test compounds

C. parvum can be transiently cultured *in vitro* using a mammalian intestinal cell line (HCT-8 cell line), while *T. gondii* can be cultured continuously *in vitro* using a diverse range of mammalian cell lines. Therefore, prior to testing the compounds’ effects on the parasites, we first analyzed their effects on the viability of uninfected HCT-8 cells. We initially tested all compounds at a final concentration of 20 µM. Among the 16 compounds tested, 7 compounds (JS-2-15, 28, 30, 31, 32, 33 and 40) reduced cell viability by less than 5% at 20 µM final concentration after 48 h of culture (Fig. 2). The remaining 9 compounds (JS-2-18, 19, 22, 25, 26, 27, 41, 43 and 44) reduced cell viability by 5–10% (Fig. 2). Based on these observations, we extrapolated that using 11 µM as the initial concentration at which to test the compounds for anti-parasitic activity would be tolerable in mammalian host cells used to culture the parasites. Therefore, all the 16 compounds were first tested *in vitro* for both anti-*Cryptosporidium* and anti-*Toxoplasma* activity at a final concentration of 11 µM.

In the case of *C. parvum*, after 72 h of culture with compound treatment, five compounds (JS-2-22, 27, 28, 30 and 44) were found to reduce parasite growth by over 60%, which was comparable to the effect of paromomycin (PMO) used as a positive control drug at a final concentration of 400 µM (Fig. 3). Three other compounds (JS-2-19, 26 and 43) reduced parasite growth by about 30%, while the remaining compounds had no significant effect on parasite growth (Fig. 3). On the other hand, treatment of *T. gondii* cultures with the compounds for 48 h showed that six compounds (JS-2-19, 28, 30, 31, 41 and 44) reduced parasite growth by over 50% (Fig. 4). Most notably, compound JS-2-44 reduced *T. gondii* growth by approximately 90%, which was comparable to the effect of atovaquone (ATQ) that was used as a positive control drug at 0.5 µM final concentration (Fig. 4).

Table 1

Reported (1-benzyl-4-triazolyl)-indole-2-carboxamides and related compounds with their overall yields, ClogP values, and IC₅₀ indices against *T. gondii* and *C. parvum* as well as cytotoxicity in mammalian HCT-8 and HFF cell lines.

Compound		Yield ^a	ClogP ^b	Parasite IC ₅₀ (μM)				Host cell IC ₅₀ (μM)		SI ^g	
Code	No.			<i>T. gondii</i>		<i>C. parvum</i>		HCT-8	HFF	<i>T. gondii</i>	<i>C. parvum</i>
				0h p.i. ^c	2h p.i. ^d	0h p.i.	2h p.i.				
JS-2-15	5a	68	3.00	NA ^e	NA	NA	NA	109.0	ND ^f		
JS-2-22	5b	58	4.14	NA	NA	12.30	12.54	101.4	ND		8.24
JS-2-18	6a	51	3.65	NA	NA	NA	NA	205.0	ND		
JS-2-25	6b	55	4.36	NA	NA	NA	NA	106.7	ND		
JS-2-26	6c	54	4.36	NA	NA	NA	NA	ND	ND		
JS-2-32	6d	58	4.36	NA	NA	NA	NA	ND	ND		
JS-2-43	6e	79	4.95	NA	NA	NA	NA	174.4	ND		
JS-2-27	7a	89	4.79	NA	NA	9.37	10.73	253.8	ND		27.09
JS-2-28	7b	67	5.50	11.63	19.23	8.32	8.59	233.4	209.4	20.07	28.05
JS-2-30	7c	76	5.50	5.43	6.32	5.05	5.86	192.70	268.0	35.49	38.16
JS-2-33	7d	65	5.50	NA	NA	NA	NA	ND	ND		
JS-2-44	7e	51	6.09	2.95 (10.55) ^h	3.24	7.63	9.12	209.7	209.1	71.08	27.48
JS-2-19	9a	36	4.54	8.51	10.60	NA	NA	ND	107.7	12.66	
JS-2-31	9b	31	5.68	7.88	12.08	NA	NA	ND	135.1	17.15	
JS-2-40	11a	24	4.23	NA	NA	NA	NA	134.8	ND		
JS-2-41	11b	18	4.36	1.94 (1.50) ^h	2.15	NA	NA	ND	167.8	86.50	
ATQ ⁱ				0.084	0.087						
PMO ^j						219.5	226.8				

^a Yield reported after purification by flash chromatography on silica.

^b Calculated with ChemDraw Professional 15.1.

^c Test compound added immediately post-infection.

^d Test compound added 2 h post-infection.

^e NA = not active in the primary compound screening.

^f ND = not done.

^g SI = selectivity index = IC₅₀ HCT-8 (or HFF)/IC₅₀ parasite (at 0 h p.i.).

^h Against *T. gondii* Type II (ME49) in HFF cells.

ⁱ ATQ = standard drug atovaquone.

^j PMO = standard drug paromomycin.

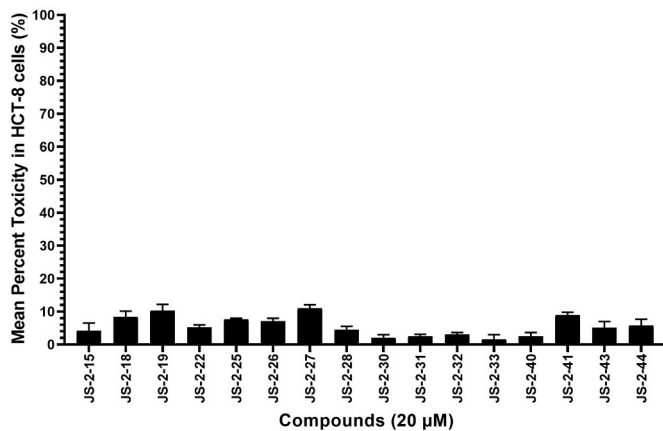


Fig. 2. Cytotoxic effects of test compounds on human ileocecal adenocarcinoma (HCT-8) cells cultured *in vitro*. Confluent monolayers of HCT-8 cells were treated with 20 μM of compound, while control cells were treated with a volume of DMSO equivalent to that used in compound-treated cells. Following 48 h of culture, the cells were analyzed for viability by a colorimetric assay using the cell proliferation reagent WST-1 (Roche). The difference in absorbance between the compound-treated cells and the DMSO-treated cells was divided by the absorbance from the DMSO-treated cells and multiplied by 100 to derive the inhibition of cell viability (%) values. The data shown represent the means from three independent experiments with standard error bars.

3.2.2. Cytotoxic IC₅₀ concentrations for compounds with anti-parasite activity

All compounds that had shown 50% or above effect of reduction of *C. parvum* growth during the initial tests were next tested at varying concentrations for cytotoxicity in uninfected HCT-8 cells in order to

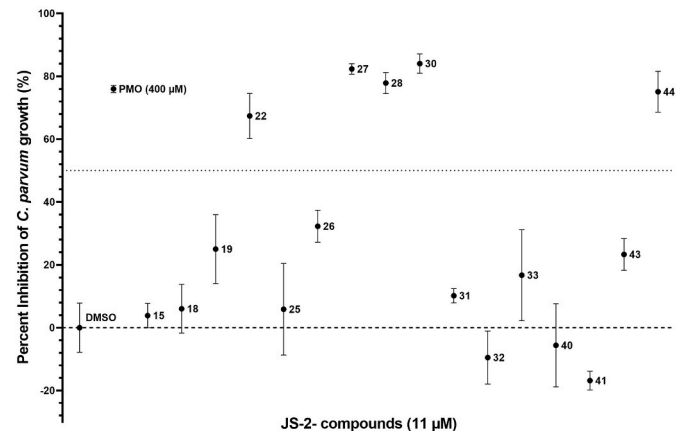


Fig. 3. Analysis of the effects of test compounds on the growth of *Cryptosporidium parvum* in human ileocecal adenocarcinoma (HCT-8) cells *in vitro*. Equal amounts of freshly excysted sporozoites of *C. parvum* were inoculated into HCT-8 cells in culture and compounds at 11 μM final concentration were added immediately after infection. Control infected cells were treated with volumes of DMSO equivalent to those used in the compound-treated cultures. Paromomycin (PMO) reconstituted in distilled sterile water was added to a separate set of wells as a positive control at 400 μM final concentration. The cultures were analyzed for parasite infectivity and proliferation by an immunofluorescence assay after 72 h of incubation. The fluorescence generated by intracellular *C. parvum* parasites was quantified by Image J software and used to calculate the mean percent parasite inhibition values of each compound. The point numerals in the image depict the last two digits of the JS-2- compound series. The data shown represents means of three independent experiments. Bars represent standard errors of the mean.

derive their cytotoxic IC₅₀ concentrations. All the compounds with

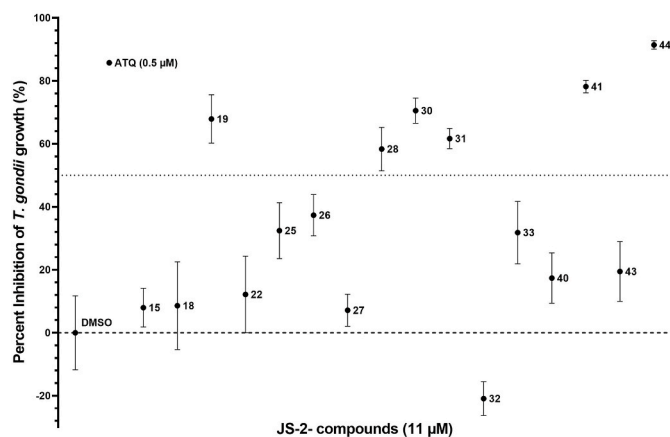


Fig. 4. Analysis of effects of the test compounds on the growth of *T. gondii* *in vitro*. Equal amounts of freshly extracted tachyzoites of *T. gondii* (constitutively expressing Yellow Fluorescent Protein) were inoculated into human foreskin fibroblasts cell line (HFF cells) in culture and compounds at 11 µM final concentration were added immediately after infection. Control infected cells were treated with volumes of DMSO equivalent to those used in the compound-treated cultures. Atovaquone reconstituted in DMSO was added to a separate set of wells as a positive control at 0.5 µM final concentration. The cultures were analyzed by fluorescence microscopy for parasite infectivity and proliferation after 48 h of incubation. Parasite fluorescence quantification was done using Image J software and the mean percent parasite inhibition values of each compound were calculated. The point numerals in the image depict the last two digits of the JS-2- compound series. The data shown represent means of three independent experiments. Bars represent standard errors of the mean.

efficacy against *C. parvum* at 11 µM depicted cytotoxic IC₅₀ concentrations in the range of 100–253.8 µM in HCT-8 cells (Table 1), suggesting that they were well tolerated by the host cells. Similarly, compounds that had depicted 50% or above reduction in *T. gondii* growth were tested at varying concentrations to derive their cytotoxic IC₅₀ concentrations in uninfected HFF cells (used for culturing *T. gondii*). The six compounds tested showed cytotoxic IC₅₀ concentrations ranging from 107.7 to 268.0 µM in HFF cells (Table 1), essentially indicating that they had no toxic effect to the HFF cells at the initial concentration (11 µM) they were tested for anti-*Toxoplasma* efficacy.

3.2.3. Compounds' anti-parasite IC₅₀ concentrations and selective indices (SI)

For all compounds that had shown anti-parasite activity at the initial testing concentration of 11 µM, a secondary screening was conducted using varying concentrations to derive their IC₅₀ concentrations against the parasites. For anti-*Cryptosporidium* screening, two formats were used: compounds were added to culture wells immediately or 2 h after inoculating the host cells with *C. parvum* sporozoites. This was meant to determine the effect of the compounds when parasites were exposed to the compounds prior to, or after infecting the host cells. We have previously observed that excysted *C. parvum* sporozoites usually invade host cells grown in 96-well plates within a 1 h window upon infection. As such, we allowed 2 h for the establishment of infection in this study. Furthermore, the 2–4 h time point has been used by many research groups (including ours) in the recent past to assess the *in vitro* effect of compounds on these parasites before and after invasion of host cells (Jumani et al., 2019; Woolsey et al., 2019; Funkhouser-Jones et al., 2020; Li et al., 2020; Ma et al., 2020; Murakoshi et al., 2020). When the cultures were analyzed at 72 h post-infection, five compounds (JS-2-22, 27, 28, 30 and 44) were found to have concentration-dependent activity of reducing *C. parvum* growth and proliferation, regardless of whether treatment started immediately or 2 h after infection of host cells (Fig. 5A–E). Their IC₅₀ concentrations ranged from 5.05 to 12.54 µM, with no significant difference between starting the treatment

immediately or 2 h after infection of the host cells (Table 1). We used paromomycin (PMO) as the positive control treatment in all *C. parvum* growth inhibition assays. Paromomycin was found to have a similar concentration-dependent effect of inhibiting *C. parvum* growth *in vitro* when added immediately or 2 h post-infection of HCT-8 cells (Fig. 5A–E), with IC₅₀ values of 219.5 and 226.8 µM, respectively. Among the five compounds with potency against *C. parvum*, JS-2-30 showed the best activity (IC₅₀ = 5.05 µM) when added immediately post infection, and had the highest selectivity index (SI) of 38.16 (Table 1). Therefore, the IC₅₀ of JS-2-30 was nearly 44-fold lower against *C. parvum* when compared directly with the reference drug PMO. When ranked in order of decreasing potency against *C. parvum*, the compounds compared as follows: JS-2-30, 44, 28, 27 and 22 (Table 1).

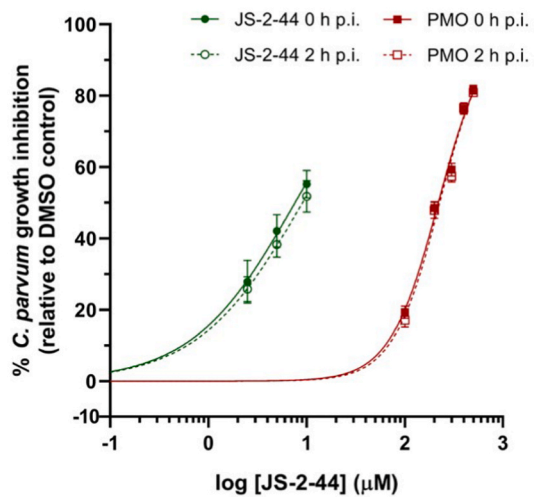
In the case of anti-*Toxoplasma* activity, when titrated at varying concentrations, compounds JS-2-19, 28, 30, 31, 41 and 44 all depicted concentration-dependent activity of reducing *T. gondii* growth *in vitro* (Fig. 6A–F). Their anti-*Toxoplasma* IC₅₀ concentrations ranged from 1.94 to 11.63 µM and 2.15–19.23 µM for treatments started immediately or 2 h post-infection, respectively (Table 1). Atovaquone, which was used as a positive control, also showed a concentration-dependent inhibitory effect on the growth of *T. gondii* parasites in HFF cells, with IC₅₀ values of 0.084 and 0.087 µM when added immediately or 2 h post-infection of host cells, respectively (Fig. 6A–F). Among the six compounds with anti-*Toxoplasma* activity, JS-2-41 was the most potent (IC₅₀ = 1.94 µM) when added immediately post infection, and showed the highest SI of 86.50. In direct comparison to the reference drug atovaquone, the IC₅₀ of JS-2-41 was 23-fold higher against *T. gondii*. Nevertheless, JS-2-41 constitutes a viable lead compound with novel scaffold that extends the current chemical space (Wu et al., 2021) and shows good promise for further development as effective agent against *T. gondii* infection. Ranking in order of decreasing potency against *T. gondii*, the compounds were listed as follows: JS-2-41, 44, 30, 31, 19, and 28 with the first three compounds having very good SI of about 86, 71, and 35 respectively (Table 1). Among the eight compounds with anti-parasite activity, only three compounds (JS-2-28, 30 and 44) were identified to be active against both *C. parvum* and *T. gondii* (Table 1). Specifically, JS-2-44 and JS-2-30 were the most potent compounds against both parasites, while JS-2-41 turned out to be the most potent compound only against *T. gondii*.

To determine IC₅₀ values of the test compounds against *C. parvum* and *T. gondii*, all test compounds were tested against the parasites at a minimum of five different concentrations. However, some compounds with high ClogP values were found to be insoluble in the culture medium at higher concentrations, which resulted in confounding results. We, therefore, excluded such unreliable data for plotting dose-response curves for these compounds. However, we ensured that a minimum of three data points are used for calculation of IC₅₀ values for all tested compounds. To the best of our knowledge, IC₅₀ values calculated using three data points are reasonably accurate especially when these data fall on the slope of the curve. Indeed, we observed a goodness-of-fit with R² values above 0.92 for all compounds in the non-linear regression model fitting using GraphPad PRISM® v8. Furthermore, a study comparing IC₅₀ values derived from a two- and 10- point assay format generated highly comparable data (r² = 0.89) and concluded that “accurate IC₅₀ predictions can be made from just two concentration points” (Turner and Charlton, 2005).

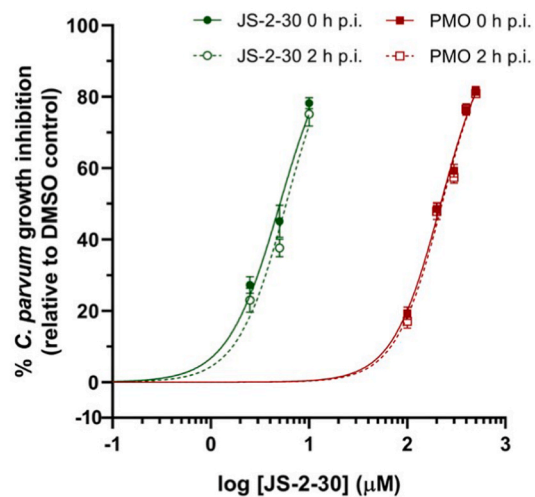
3.2.4. Compounds with anti-*Toxoplasma* potency decrease parasite cyst counts in the brains of infected rats

Having identified the compounds that had *in vitro* activity against *T. gondii*, we endeavored to test their *in vivo* efficacy in eliminating the parasite brain cysts in infected Brown Norway (BN) rats with confirmed parasite cyst burden. BN rats are susceptible to *T. gondii* infection, and this has been shown to lead to formation of parasite cysts in the brain after about 3–4 weeks post-infection in the case of Type II *T. gondii* infection (Dubey et al., 2016). Therefore, we maintained BN rats infected with Type II *T. gondii* (ME49) for 5 weeks and then sacrificed

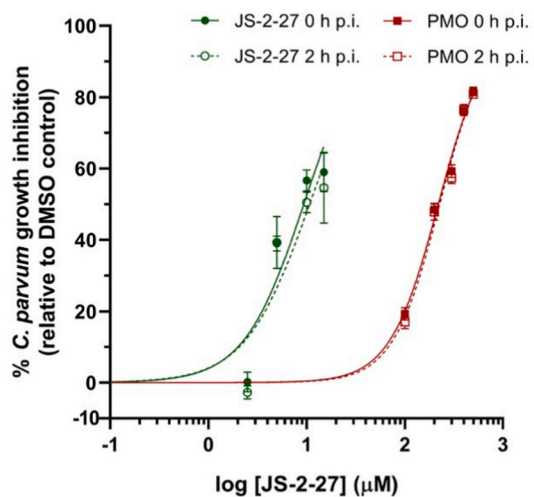
A



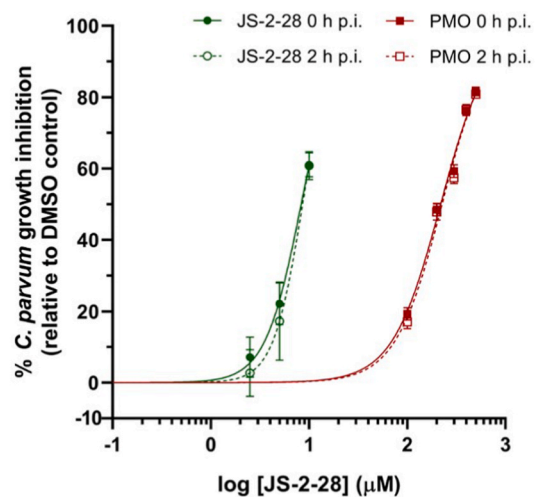
B



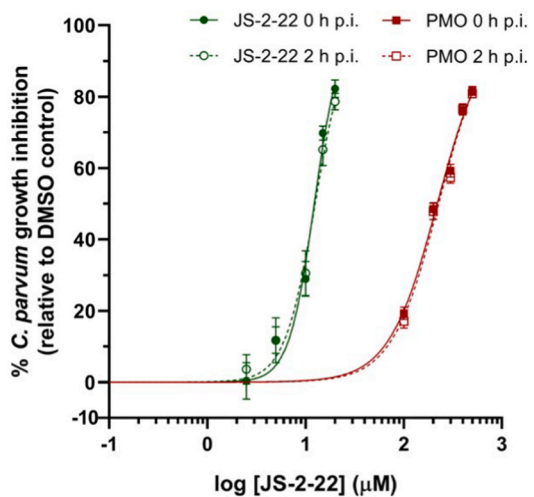
C



D



E



(caption on next page)

Fig. 5. Effect of varying concentrations of the test compounds on the growth of *C. parvum* in HCT-8 cells. Equal amounts of freshly excysted sporozoites of *C. parvum* were inoculated into HCT-8 cells in culture and varying concentrations of (A) JS-2-44, (B) JS-2-30, (C) JS-2-27, (D) JS-2-28 and (E) JS-2-22 were added at the time of infection (green solid line) or added 2 h post-infection (p.i.) (green dashed line). Control infected cells were treated immediately p.i. with volumes of DMSO equivalent to those used in the compound-treated cultures. Varying concentrations of paromomycin (PMO) added at infection (red solid line) or 2 h p.i. (red dashed line) served as the positive control. The cultures were analyzed for parasite infectivity and proliferation by an immunofluorescence assay after 72 h of culture. The fluorescence generated by intracellular *C. parvum* parasites was quantified and used to calculate the mean percent parasite inhibition values of each compound concentration relative to the DMSO-treated controls. The data shown represent means of three independent experiments. Bars represent standard errors of the mean. (For interpretation of the references to colour in this figure legend, the reader is referred to the web version of this article.)

two of the infected rats to confirm presence of cysts in their brains. On average, each rat's brain was found to harbor about 150 *T. gondii* cysts of varying sizes (Fig. 7A). After confirmation of the presence of cysts in the infected rats, we commenced daily (for a total of 14 days) treatment of rats using two selected compounds (JS-2-41 and JS-2-44) that had shown the highest potency against *T. gondii* *in vitro*. Atovaquone treatment was included as a positive control drug. One day after completing treatment, the rats were sacrificed and the number of *T. gondii* cysts in their brains enumerated. We found that, on average, the rats in the untreated group had about 200 cysts per brain (Fig. 7B). Interestingly treatment with compound JS-2-41 and JS-2-44, resulted in a significant reduction in cysts number, down to an average of about 20 cysts per brain (Fig. 7B), which was a 10-fold decrease when compared to the untreated rats. Atovaquone treatment was also found to be effective in decreasing cysts burden to a similar extent as compounds JS-2-41 and JS-2-44. Because, we had used Type I *T. gondii* (RH) for the anti-*Toxoplasma* compound activity assays, while Type II *T. gondii* (ME49) was used for the *in vivo* efficacy assays, we endeavored to also determine the *in vitro* anti-Type II activity of JS-2-41 and JS-2-44 compounds that showed the highest efficacy *in vivo*. Both compounds depicted concentration-dependent activity comparable to atovaquone, against Type II *T. gondii* (ME49) (Fig. 8), consistent with what was observed with Type I *T. gondii* assay. However, while JS-2-41 had similar IC₅₀ concentration against both Type I (1.94 μM) and Type II (1.50 μM), JS-2-44 had higher IC₅₀ concentration against Type II (10.55 μM) than Type I (2.95 μM). Nevertheless, *in vivo*, both JS-2-41 and JS-2-44 compounds showed similar potency.

4. Discussion

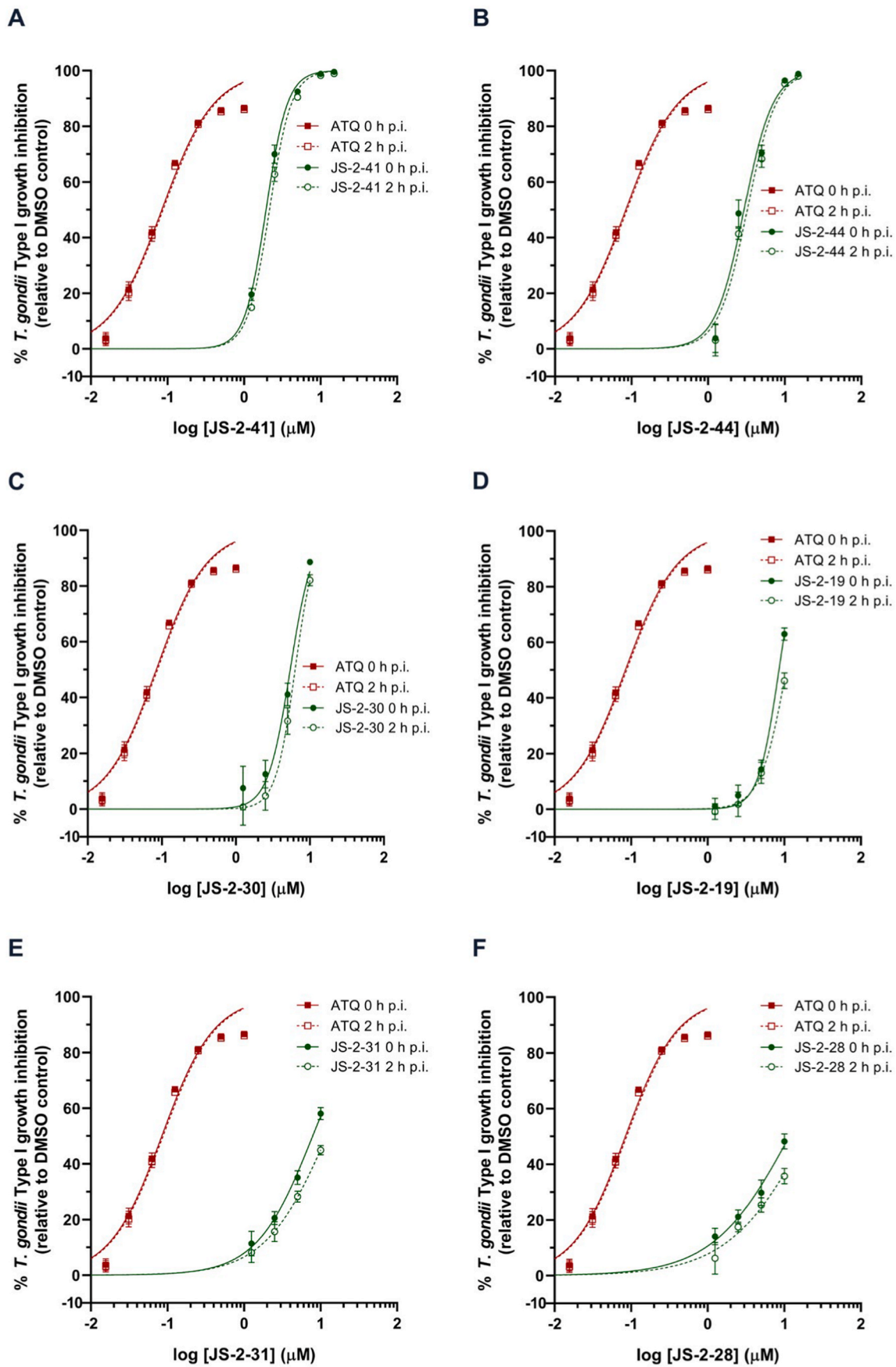
Cryptosporidium and *Toxoplasma* are highly prevalent zoonotic protozoan parasites with worldwide distribution, but for which no completely effective therapeutic agents exist. Herein, we present structural derivatives obtained through modification of the highly active antimycobacterial lead compound JS-2-02 (Stec et al., 2016; Lun et al., 2019) and showcase that the new compounds possess significant efficacy against *T. gondii* and appreciable activity against *C. parvum*. Given the fact that the lead compound JS-2-02 contains the indole skeleton, which is designated as a privileged scaffold (Welsch et al., 2010), as well as knowing the prominent role of triazole ring in medicinal chemistry (Zhou and Wang, 2012), we set off to synthesize (1-benzyl-4-triazolyl)-indole-2-carboxamides as prospective antiparasitic agents. Interestingly, among the synthesized derivatives, compounds representing the 4,6-dichloro series **7a-e**, i.e. JS-2-27, 28, 30, 33 and 44 showed the desired antiparasitic activity as opposed to their 4,6-difluoro counterparts **6a-e**, i.e. JS-2-18, 25, 26, 32 and 43 (Scheme 1, Table 1). This suggested that the presence of chlorine atoms plays a crucial role in the bioactivity of this subset of compounds. Given the substantial differences in various properties such as electronegativity, polarity, lipophilicity, and size between the lighter fluorine and the heavier chlorine atoms (Wilcken et al., 2013), organic molecules differing with respect to those two substituents will very often show distinctive activities as well as physicochemical and ADMET properties such as water solubility, permeability, etc. In particular, a compound's lipophilicity plays crucial role for the molecule to effectively penetrate the relatively complex parasite's pellicle (i.e. outer covering) composed of a plasmalemma and two tightly apposed membranes that form an inner membrane complex

(Dubey et al., 1998). Thus, the increased lipophilicity of the 4,6-dichloro indole series very likely determines the overall bioactivity of those compounds. Of note is the fact that the presented compounds show very encouraging drug-like properties (Molinspiration Cheminformatics, 2022) of orally bioavailable drugs as none of the molecules violates the Veber's Rule (Veber et al., 2002) and just few of them (JS-2-28, 30, 31, 33 and 44) violate only one postulate (ClogP <5) of the Lipinski's Rule of Five (Lipinski, 2000; Lipinski et al., 2001). High ClogP value and thus enhanced lipophilicity plays not only crucial role for drugs' absorption but also penetration across the blood-brain barrier and thus enhanced drugs' distribution within the brain, an organ where often the persistent cysts of *T. gondii* are formed.

The presence and distribution of the chlorine atoms on the benzyl ring attached to the triazole moiety also seems to play an important role in the antiparasitic activity. Compound **7a** (JS-2-27) bearing the unsubstituted benzyl ring showed appreciable activity only against *C. parvum* whereas the *o*-chloro derivative **7b** (JS-2-28) displayed only weak anti-*T. gondii* activity, but with improved anti-*C. parvum* activity when compared to the parent compound **7a**. On the other hand, *m*-chloro derivative **7c** (JS-2-30) yielded the most potent compound against *C. parvum* and fairly active compound against *T. gondii*. On the contrary, the *p*-chloro analog **7d** (JS-2-33) turned out to be inactive against both parasites. However, the activity was restored with the *m,p*-dichloro derivative **7e** (JS-2-44), which yielded the second most potent compound against *T. gondii* (after compound **11b**; JS-2-41) and *C. parvum* (after compound **7c**; JS-2-30). This trend clearly indicates the importance of substitution on the *meta* position of the benzyl ring for the desired antiparasitic activity. Interestingly, the *m,p*-dichlorobenzyl motif is also found in another chemotype with high anticryptosporidial activity reported in the literature (Oboh et al., 2021). Both of the 1-adamantyl counterparts **9a** (JS-2-19) and **9b** (JS-2-31) showed activity only against *T. gondii*. This result is consistent with our previous report that showed some 1- and 2-adamantyl benzoyl carbamates to selectively inhibit the growth of *T. gondii* with comparable IC₅₀ indices (Li et al., 2020). Extension of the project to the synthesis of (1-adamantyl)-4-phenyl-triazoles provided compounds **11a** (JS-2-40) and **11b** (JS-2-41) with the latter derivative being the most potent compound against *T. gondii*. Given the presence of a masked aldehyde group in **11b**, thus the ease for medicinal chemistry structure elaboration, further expansion of this project is currently underway.

Importantly, the compounds (JS-2-28, JS-2-30, and JS-2-44) that were found to have efficacy against both *T. gondii* and *C. parvum* at low micromolar concentrations also depicted good safety margins (selectivity indices) in human host cells that were used to culture the parasites (Table 1). This implies the aforementioned compounds are effective against the parasites at concentrations that are not toxic to the host cells. In the case of *C. parvum*, paromomycin was used as a positive control drug and displayed an *in vitro* anti-*Cryptosporidium* IC₅₀ concentration of 219.5 μM. Paromomycin has been shown to be non-toxic to human cells at concentrations higher than 1000 μM (Downey et al., 2008; Gargala et al., 2000). Comparatively, the four compounds (JS-2-27, 28, 30 and 44) that were identified in this study to be active against *C. parvum* had much lower IC₅₀ values (9.37, 8.32, 5.05 and 7.63 μM, respectively) and better selectivity indices than paromomycin, implying their promising efficacy and safety profile.

On the other hand, for testing compounds against *T. gondii*, atovaquone was used as a positive control and showed an *in vitro* IC₅₀



(caption on next page)

Fig. 6. Effect of varying concentrations of test compounds on the growth of *Toxoplasma gondii* in human foreskin fibroblasts (HFF) cells. Equal amounts of freshly extracted tachyzoites of *T. gondii* (constitutively expressing yellow fluorescent protein) were inoculated into HFF cells in culture and varying concentrations of compounds (A) JS-2-41, (B) JS-2-44, (C) JS-2-30, (D) JS-2-19, (E) JS-2-31, (F) JS-2-28 were added immediately (green solid line) or 2 h post-infection (p.i.) (green dashed line). Control infected cells were treated immediately p.i. with volumes of DMSO equivalent to those used in the compound-treated cultures. Atovaquone (ATQ) was added at varying concentrations to a separate set of wells immediately after infection (red solid line) or 2 h p.i. (red dashed line) as a positive control. The cultures were analyzed for parasite infectivity and proliferation after 48 h of incubation by fluorescence microscopy to measure parasite fluorescence. The fluorescence generated by *T. gondii* was quantified using Image J software and used to calculate the mean percent parasite inhibition values of each compound concentration relative to the DMSO-treated controls. The data shown represent means of three independent experiments. Bars represent standard errors of the mean. (For interpretation of the references to colour in this figure legend, the reader is referred to the web version of this article.)

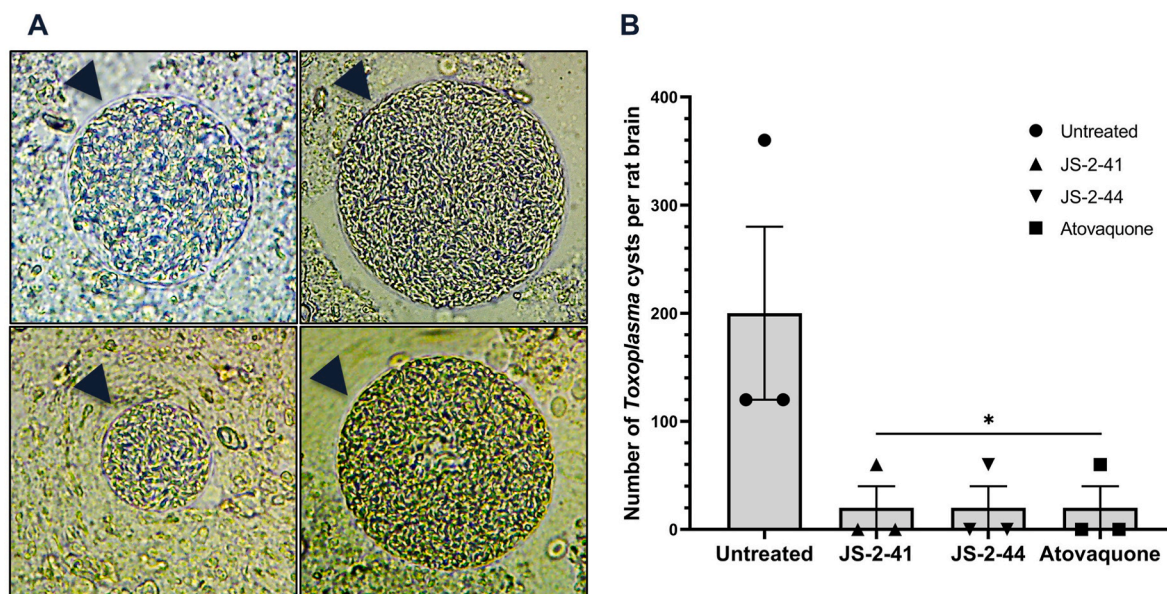


Fig. 7. *In vivo* efficacy of the test compounds against *T. gondii* Type II (ME49) cysts in rats' brains. Male Brown Norway rats were each inoculated intramuscularly with 5×10^4 freshly isolated *T. gondii* ME49 strain tachyzoites and maintained for 4 weeks to develop brain cysts, after which each group ($n = 3$) of infected rats was treated by intraperitoneal injection with compound JS-2-41 (3 mg/kg), JS-2-44 (4 mg/kg), or atovaquone (5 mg/kg) daily for 14 days. The control group of infected rats received an equivalent volume of DMSO solvent. Following treatment, rat brains were harvested and (A) the number of *T. gondii* cysts of varying sizes (indicated by arrow heads in the representative images) per rat brain were (B) enumerated and are shown as the mean number from 3 infected rats per treatment. Bars represent standard errors of the mean with levels of statistical significance as compared to the untreated control indicated by asterisk (*, $P < 0.05$; one-way ANOVA and Dunnett's multiple-comparison test).

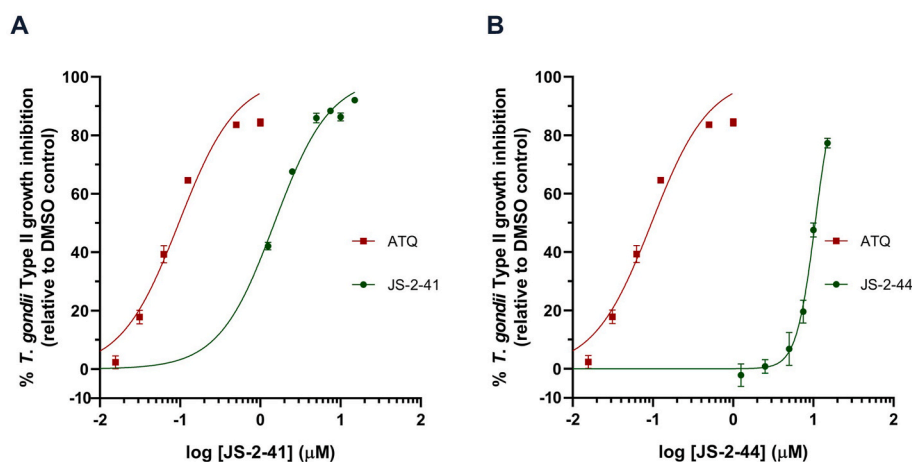


Fig. 8. Effect of varying concentrations of test compounds on the growth of *Toxoplasma gondii* Type II (ME49) in human foreskin fibroblasts (HFF) cells. Equal amounts of freshly extracted tachyzoites of *T. gondii* (constitutively expressing luciferase protein - Fluc) were inoculated into HFF cells in culture and varying concentrations of compounds (A) JS-2-41 or (B) JS-2-44, were added immediately post-infection (green line). Control infected cells were treated immediately post-infection with volumes of DMSO equivalent to those used in the compound-treated cultures. Varying concentrations of ATQ added at the time of infection (red line) served as the positive control. The cultures were analyzed for parasite infectivity and proliferation after 48 h using a luciferase reporter gene assay. The luminescence generated by *T. gondii* luciferase activity was recorded and used to calculate the mean percent parasite inhibition values of each compound concentration relative to the DMSO-treated controls. Indicated values represent means from three independent experiments. Bars represent standard deviations of the

mean. (For interpretation of the references to colour in this figure legend, the reader is referred to the web version of this article.)

concentration of $0.087 \mu\text{M}$ against *T. gondii*. Atovaquone has been shown to be toxic to human host cells *in vitro* at a concentration that is 10-fold higher than its effective parasite inhibitory concentration (Araujo et al.,

1991). Comparatively, all the compounds that were found to be active *in vitro* against *T. gondii* (JS-2-19, 28, 30, 31, 41 and 44), had anti-*Toxoplasma* IC_{50} values 11.6–86.5-fold lower than their cytotoxic IC_{50}

concentrations. Those results suggest that the aforementioned test compounds are efficacious with a wider safety margin than atovaquone. Such characteristic of new hit molecules is especially important in addressing the problems of toxicity and hypersensitivity that are associated with currently licensed medications used for the treatment of toxoplasmosis in humans (McLeod et al., 2006; Rajapakse et al., 2013; Montazeri et al., 2015).

Rats, like immunocompetent humans, are relatively resistant to clinical toxoplasmosis and develop a subclinical chronic infection that results in the development of cysts in brain, eyes, and muscle tissues (Dubey et al., 2016). Currently licensed drugs against *T. gondii* are not very effective at eliminating the cyst stage of the parasite, implying that they cannot completely clear the infection in chronically infected individuals. By evaluating *in vivo* JS-2-41 and JS-2-44 we found that these compounds were effective in reducing (by over 90%) the number of *Toxoplasma* cysts in the brain of infected rats just after 14 days of treatment. Considering that we only tested at a single dose, it can be postulated that higher doses of those two compounds, and prolonged treatment could potentially completely eliminate the encysted stages of *T. gondii*. Given the promising *in vitro* safety margin that we observed for those compounds, it is likely that both molecules could be well tolerated *in vivo* at higher doses. Further evaluation of the lead compounds in terms of various ADMET properties such as hERG potassium channel inhibition, mutagenicity, induction/inhibition of CYP450 isoforms, metabolic stability/half-life, permeability, will provide useful data for advancing those compounds.

5. Conclusions

Novel (1-benzyl-4-triazolyl)-indole-2-carboxamides and (1-adamantyl)-4-phenyl-triazoles have been prepared and evaluated for activity against *T. gondii* and *C. parvum*. Several of the analogs presented herein showed appreciable antiparasitic activity with JS-2-30, JS-2-44, and JS-2-41 being the most active derivatives in the entire series. While JS-2-30 and JS-2-44 were active against both parasites at low micromolar concentrations (IC₅₀ ranging from 2.95 to 7.63 μM), JS-2-41 selectively inhibited the growth of *T. gondii* with an IC₅₀ of 1.94 μM and SI value above 86. The most active derivative in this set against *C. parvum* was JS-2-30 with an IC₅₀ of 5.05 μM, which is nearly 44-fold lower value in comparison with the reference drug PMO. On the other hand, the most active derivative in this set against *T. gondii* was JS-2-41 with an IC₅₀ of 1.94 μM, which is 23-fold higher value in comparison with the reference drug ATQ. Furthermore, JS-2-44 and JS-2-41 were also active *in vivo* as assessed by their ability to significantly reduce the number of *T. gondii* cysts in the brain of infected rats. Overall, these results along with good drug-likeness of the compounds provide further basis for structure modification of JS-2-44 and JS-2-41 in search of novel antiparasitic agents.

6. Ethics

All experiments involving the use of animals in this study were carried out in strict compliance with the recommendations and guidelines of the United States Department of Agriculture Animal Welfare Act and the National Institute of Health Public Health Service Policy on the Humane Care and Use of Animals. The protocol number 18151 and 21091 used were approved by the University of Illinois Institutional Animal Care and Use Committee for conducting research with rats and calves, respectively. All efforts were made to reduce the pain and suffering of animals.

Declaration of competing interest

The authors declare that they have no known competing financial interests or personal relationships that could have appeared to influence the work reported in this paper.

Acknowledgements

This study was supported in part by funds from the University of Illinois at Urbana-Champaign, USA, to WHW. JS wishes to acknowledge Marshall B. Ketchum University COP for startup funds and faculty travel stipend. GMG, AGH, and JS acknowledge Chicago State University (CSU) COP and CSU CTRE (Seed Grant) for generous financial support of this project. The unlimited access to the NMR facility (JEOL 400) in the Department of Chemistry at CSU is acknowledged. Mr. Daniel Pietryla is acknowledged for providing technical assistance in the laboratory. We thank Dr. Shichun Lun and Professor William R. Bishai (Johns Hopkins University) for initial screening of the compounds against *Mycobacterium tuberculosis*.

Appendix A. Supplementary data

Supplementary data to this article can be found online at <https://doi.org/10.1016/j.ijpddr.2022.04.001>.

References

- Andrews, K.T., Fisher, G., Skinner-Adams, T.S., 2014. Drug repurposing and human parasitic Protozoan diseases. *Int. J. Parasitol. Drugs Drug Resist.* 4 (2), 95–111. <https://doi.org/10.1016/j.ijpddr.2014.02.002>.
- Araujo, F.G., Huskinson, J., Remington, J.S., 1991. Remarkable *in vitro* and *in vivo* activities of the hydroxynaphthoquinone 566C80 against tachyzoites and tissue cysts of *Toxoplasma gondii*. *Antimicrob. Agents Chemother.* 35 (2), 293–299. <https://doi.org/10.1128/aac.35.2.293>.
- Arrowood, M.J., Sterling, C.R., 1987. Isolation of *Cryptosporidium* oocysts and sporozoites using discontinuous sucrose and isopycnic percoll gradients. *J. Parasitol.* 73 (2), 314–319. <https://doi.org/10.2307/3282084>.
- Austin, C.P., Mount, B.A., Colvis, C.M., 2021. Envisioning an actionable research agenda to facilitate repurposing of off-patent drugs. *Nat. Rev. Drug Discov.* 20, 723–724. <https://doi.org/10.1038/d41573-021-00090-y>.
- Baek, K.-H., Phan, T.-N., Malwal, S.R., Lee, H., Li, Z.-H., Moreno, S.N.J., Oldfield, E., No, J.H., 2022. *In vivo* efficacy of SQ109 against *Leishmania donovani*, *trypanosoma* spp. and *Toxoplasma gondii* and *in vitro* activity of SQ109 metabolites. *Biomedicines* 10, 670. <https://doi.org/10.3390/biomedicines10030670>.
- Bellini, V., Swale, C., Brenier-Pinchart, M.P., Pezier, T., Georgeault, S., Laurent, F., Hakimi, M.A., Bougdour, A., 2020. Target identification of an antimarial oxaborole identifies AN13762 as an alternative chemotype for targeting CPSF3 in apicomplexan parasites. *iScience* 23 (12), 101871. <https://doi.org/10.1016/j.isci.2020.101871>.
- Bolia, R., 2020. Nitazoxanide: jack of all, master of none? *Indian J. Pediatr.* 87, 4–5. <https://doi.org/10.1007/s12098-019-03131-y>.
- Boyom, F.F., Fokou, P.V.T., Tchokouaha, L.R.Y., Spangenberg, T., Mfopa, A.N., Kouipou, R.M.T., Mbouna, C.J., Donkeng Donfack, V.F., Zollo, P.H.A., 2014. Repurposing the open access malaria box to discover potent inhibitors of *Toxoplasma gondii* and *Entamoeba histolytica*. *Antimicrob. Agents Chemother.* 58, 5848–5854. <https://doi.org/10.1128/AAC.02541-14>.
- Castro-Filice, L.S., Barbosa, B.F., Angeloni, M.B., Silva, N.M., Gomes, A.O., Alves, C.M.O. S., Silva, D.A.O., Martins-Filho, O.A., Santos, M.C., Mineo, J.R., Ferro, E.A.V., 2014. Azithromycin is able to control *Toxoplasma gondii* infection in human villous explants. *J. Transl. Med.* 12, 132. <https://doi.org/10.1186/1479-5876-12-132>.
- Centers for Disease Control and Prevention (CDC). Zoonotic diseases. <https://www.cdc.gov/onehealth/basics/zoonotic-diseases.html>. (Accessed 17 February 2022).
- Centers for Disease Control and Prevention (CDC). Parasites - toxoplasmosis (*Toxoplasma* infection). <https://www.cdc.gov/parasites/toxoplasmosis/index.html>. (Accessed 17 February 2022).
- Centers for Disease Control and Prevention (CDC). Parasites - Cryptosporidium. <https://www.cdc.gov/parasites/crypto/index.html>. (Accessed 17 February 2022).
- Centers for Disease Control and Prevention (CDC). Guidelines for the prevention and treatment of opportunistic infections in adults and adolescents with HIV. HIV recommendations from the centers for disease control and prevention, the National Institutes of Health, and the HIV Medicine Association Of The Infectious Diseases Society of America. <https://clinicalinfo.hiv.gov/en/guidelines/adult-and-adolesc-ent-opportunistic-infection/toxoplasma-gondii-encephalitis>. (Accessed 17 February 2022).
- Current, W.L., 1990. Techniques and laboratory maintenance of *Cryptosporidium*. In: Dubey, J.P., Speer, C.A., Fayer, R. (Eds.), *Cryptosporidiosis of Man and Animals*. CRC Press, Boca Raton, Fla.
- Downey, A.S., Chong, C.R., Graczyk, T.K., Sullivan, D.J., 2008. Efficacy of pyriminium pamoate against *Cryptosporidium parvum* infection *in vitro* and in a neonatal mouse model. *Antimicrob. Agents Chemother.* 52 (9), 3106–3112. <https://doi.org/10.1128/AAC.00207-08>.
- Dubey, J.P., Ferreira, L.R., Alsaad, M., Verma, S.K., Alves, D.A., Holland, G.N., McConkey, G.A., 2016. Experimental toxoplasmosis in rats induced orally with eleven strains of *Toxoplasma gondii* of seven genotypes: tissue tropism, tissue cyst size, neural lesions, tissue cyst rupture without reactivation, and ocular lesions. *PLoS One* 11 (5), e0156255. <https://doi.org/10.1371/journal.pone.0156255>.

- Dubey, J.P., Lindsay, D.S., Speer, C.A., 1998. Structures of *Toxoplasma gondii* tachyzoites, bradyzoites, and sporozoites and biology and development of tissue cysts. *Clin. Microbiol. Rev.* 11 (2), 267–299. <https://doi.org/10.1128/CMR.11.2.267>.
- Flegr, J., Prandota, J., Sovicková, M., Israeli, Z.H., 2014. Toxoplasmosis – a global threat. Correlation of latent toxoplasmosis with specific disease burden in a set of 88 countries. *PLoS One* 9 (3), e92023. <https://doi.org/10.1371/journal.pone.0090203>.
- Fritzler, J.M., Zhu, G., 2012. Novel anti-cryptosporidium activity of known drugs identified by high-throughput screening against parasite fatty acyl-CoA binding protein (ACBP). *J. Antimicrob. Chemother.* 67 (3), 609–617. <https://doi.org/10.1093/jac/dkr516>.
- Funkhouser-Jones, L.J., Ravindran, S., Sibley, L.D., 2020. Defining stage-specific activity of potent new inhibitors of *Cryptosporidium parvum* growth *in vitro*. *mBio* 11 (2). <https://doi.org/10.1128/mBio.00052-20> e00052-20.
- Gargala, G., Delaunay, A., Li, X., Brassieur, P., Favennec, L., Ballet, J.J., 2000. Efficacy of nitazoxanide, tizoxanide and tizoxanide glucuronide against *Cryptosporidium parvum* development in sporozoite-infected HCT-8 enterocytic cells. *J. Antimicrob. Chemother.* 46 (1), 57–60. <https://doi.org/10.1093/jac/46.1.57>.
- Gerace, E., Di Marco Lo Presti, V., Biondo, C., 2019. *Cryptosporidium* infection: epidemiology, pathogenesis, and differential diagnosis. *Eur. J. Microbiol. Immunol.* (Bp). 9 (4), 119–123. <https://doi.org/10.1556/1886.2019.00019>.
- Gubbels, M.J., Li, C., Striepen, B., 2003. High-throughput growth assay for *Toxoplasma gondii* using yellow fluorescent protein. *Antimicrob. Agents Chemother.* 47 (1), 309–316. <https://doi.org/10.1128/AAC.47.1.309-316.2003>.
- Guo, F., Zhang, H., McNair, N.N., Mead, J.R., Zhu, G., 2018. The existing drug vorinostat as a new lead against cryptosporidiosis by targeting the parasite histone deacetylases. *J. Infect. Dis.* 217 (7), 1110–1117. <https://doi.org/10.1093/infdis/jix689>.
- Himo, F., Lovell, T., Hilgraf, R., Rostovtsev, V.V., Noodleman, L., Sharpless, K.B., Fokin, V.V., 2005. Copper(I)-Catalyzed synthesis of azoles. DFT study predicts unprecedented reactivity and intermediates. *J. Am. Chem. Soc.* 127 (1), 210–216. <https://doi.org/10.1021/ja0471525>.
- Jeffers, V., Tampaki, Z., Kim, K., Sullivan Jr., W.J., 2018. A latent ability to persist: differentiation in *Toxoplasma gondii*. *Cell. Mol. Life Sci.* 75 (13), 2355–2373. <https://doi.org/10.1007/s00018-018-2808-x>.
- Jumani, R.S., Hasan, M.M., Stebbins, E.E., Donnelly, L., Miller, P., Klopfer, C., Bessoff, K., Teixeira, J.E., Love, M.S., McNamara, C.W., Huston, C.D., 2019. A suite of phenotypic assays to ensure pipeline diversity when prioritizing drug-like *Cryptosporidium* growth inhibitors. *Nat. Commun.* 10 (1), 1862. <https://doi.org/10.1038/s41467-019-09880-w>.
- Kale, M.A., Shamkuwar, P.B., Mourya, V.K., Deshpande, A.B., Shelke, P.A., 2022. Drug repositioning: a unique approach to refurbish drug discovery. *Curr. Drug Discov. Technol.* 19 (1), e140122192307 <https://doi.org/10.2174/1570163818666210316114331>.
- Kuhlenschmidt, T.B., Rutaganira, F.U., Long, S., Tang, K., Shokat, K.M., Kuhlenschmidt, M.S., Sibley, L.D., 2016. Inhibition of calcium-dependent protein kinase 1 (CDPK1) *in vitro* by pyrazolopyrimidine derivatives does not correlate with sensitivity of *Cryptosporidium parvum* growth in cell culture. *Antimicrob. Agents Chemother.* 60 (1), 570–579. <https://doi.org/10.1128/AAC.01915-15>.
- Li, K., Wang, Y., Yang, G., Byun, S., Rao, G., Shoen, C., Yang, H., Gulati, A., Crick, D.C., Cynamon, M., Huang, G., Docampo, R., No, J.H., Oldfield, E., 2015. Oxa, thia, heterocycle, and carborene analogues of SQ109: bacterial and Protozoal cell growth inhibitors. *ACS Infect. Dis.* 1 (5), 215–221. <https://doi.org/10.1021/acsinfecdis.5b00026>.
- Li, K., Grooms, G.M., Khan, S.M., Garcia Hernandez, A., Witola, W.H., Stec, J., 2020. Novel acyl carbamates and acyl/diacyl ureas show *in vitro* efficacy against *Toxoplasma gondii* and *Cryptosporidium parvum*. *Int. J. Parasitol. Drugs Drug Resist.* 14, 80–90. <https://doi.org/10.1016/j.ijpdr.2020.08.006>.
- Lipinski, C.A., 2000. Drug-like properties and the causes of poor solubility and poor permeability. *J. Pharmacol. Toxicol. Methods* 44 (1), 235–249. [https://doi.org/10.1016/S1056-8719\(00\)00107-6](https://doi.org/10.1016/S1056-8719(00)00107-6).
- Lipinski, C.A., Lombardo, F., Dominy, B.W., Feeney, P.J., 2001. Experimental and computational approaches to estimate solubility and permeability in drug discovery and development settings. *Adv. Drug Deliv. Rev.* 46 (1–3), 3–26. [https://doi.org/10.1016/S0169-409X\(00\)00129-0](https://doi.org/10.1016/S0169-409X(00)00129-0).
- Lun, S., Guo, H., Onajole, O.K., Pieroni, M., Gunosewoyo, H., Chen, G., Tipparaju, S.K., Ammerman, N.C., Kozikowski, A.P., Bishai, W.R., 2013. Indoleamides are active against drug-resistant *Mycobacterium tuberculosis*. *Nat. Commun.* 4, 2907. <https://doi.org/10.1038/ncomms3907>.
- Lun, S., Tasneen, R., Chaira, T., Stec, J., Onajole, O.K., Yang, T.J., Cooper, C.B., Mdluli, K., Converse, P., Nuermberger, E., Raj, V.S., Kozikowski, A.P., Bishai, W.R., 2019. Advancing the therapeutic potential of indoleamides for Tuberculosis. *Antimicrob. Agents Chemother.* 63 (7) <https://doi.org/10.1128/AAC.00343-19> e00343-00319.
- Ma, J., Guo, F., Jin, Z., Geng, M., Ju, M., Ravichandran, A., Oruguntla, R., Smith, L., Zhu, G., Zhang, H., 2020. Novel antiparasitic activity of the antifungal lead occidiofungin. *Antimicrob. Agents Chemother.* 64 (8) <https://doi.org/10.1128/AAC.00244-20> e00244-20.
- Malwal, S., Baek, K.-H., Phan, T.-N., Lee, H., Li, Z.-H., Moreno, S.N.J., No, J.H., Oldfield, E., 2021. Lipid Transporters: from Bacteria, Protozoa, Fungi and Plants, to Mice and Men. *ChemRxiv*, Cambridge. Cambridge Open Engage. <https://chemrxiv.org/engage/chemrxiv/article-details/60c758529abda20866f8e8b8>.
- Malwal, S.R., Oldfield, E., 2022. Mycobacterial membrane protein large 3-like-family proteins in bacteria, protozoa, fungi, plants, and animals: a bioinformatics and structural investigation. *Proteins* 90 (3), 776–790. <https://doi.org/10.1002/prot.26273>.
- McLeod, R., Khan, A., Nobel, G., Latkany, P., Jalbrzikowski, J., Boyer, K., 2006. Severe sulfadiazine hypersensitivity in a child with reactivated congenital toxoplasmic chorioretinitis. *Pediatr. Infect. Dis. J.* 25 (3), 270–272. <https://doi.org/10.1097/01.inf.0000202070.59190.9a>.
- Molinspiration Cheminformatics. Calculated by using molinspiration, a free web-based software. <https://www.molinspiration.com/>. (Accessed 17 February 2022).
- Montazeri, M., Daryani, A., Ebrahimzadeh, M., Ahmadpour, E., Sharif, M., Sarvi, S., 2015. Effect of propranolol alone and in combination with pyrimethamine on acute murine toxoplasmosis. *Jundishapur J. Microbiol.* 8 (9), e22572 <https://doi.org/10.5812/jjm.22572>.
- Murakoshi, F., Bando, H., Sugi, T., Adeyemi, O.S., Nonaka, M., Nakaya, T., Kato, K., 2020. Nullscript inhibits *Cryptosporidium* and *Toxoplasma* growth. *Int. J. Parasitol. Drugs Drug Resist.* 14, 159–166. <https://doi.org/10.1016/j.ijpdr.2020.10.004>.
- Oboh, E., Schubert, T.J., Teixeira, J.E., Stebbins, E.E., Miller, P., Philo, E., Thakellapalli, H., Campbell, S.D., Griggs, D.W., Huston, C.D., Meyers, M.J., 2021. Optimization of the urea linker of triazolopyridazine MMV665917 results in a new anticryptosporidial lead with improved potency and predicted hERG safety margin. *J. Med. Chem.* 64 (15), 11729–11745. <https://doi.org/10.1021/acs.jmedchem.1c01136>.
- Onajole, O.K., Pieroni, M., Tipparaju, S.K., Lun, S., Stec, J., Chen, G., Gunosewoyo, H., Guo, H., Ammerman, N.C., Bishai, W.R., Kozikowski, A.P., 2013. Preliminary structure-activity relationships and biological evaluation of novel antitubercular indolecarboxamide derivatives against drug-susceptible and drug-resistant *Mycobacterium tuberculosis* strains. *J. Med. Chem.* 56 (10), 4093–4103. <https://doi.org/10.1021/jm4003878>.
- Palencia, A., Bougdour, A., Brenier-Pinchart, M.-P., Touquet, B., Bertini, R.-L., Sensi, C., Gay, G., Voltaire, J., Jossierand, V., Easom, E., Freund, Y.R., Pelloux, H., Rosenthal, P.J., Cusack, S., Hakimi, M.-A., 2017. Targeting *Toxoplasma gondii* CPSF3 as a new approach to control toxoplasmosis. *EMBO Mol. Med.* 9 (3), 385–394. <https://doi.org/10.15252/emmm.201607370>.
- Rajapakse, S., Krishan Shivantham, M., Samaranyake, N., Rodrigo, C., Deepika Fernando, S., 2013. Antibiotics for human toxoplasmosis: a systematic review of randomized trials. *Pathog. Glob. Health* 107 (44), 162–169. <https://doi.org/10.1179/2047773213Y.0000000094>.
- Rottmann, M., McNamara, C., Yeung, B.K., Lee, M.C., Zou, B., Russell, B., Seitz, P., Plouffe, D.M., Dharia, N.V., Tan, J., Cohen, S.B., Spencer, K.R., González-Pérez, G.E., Lakshminarayana, S.B., Goh, A., Suwanarusk, R., Jegla, T., Schmitt, E.K., Beck, H.P., Brun, R., Nosten, F., Renia, L., Dartois, V., Keller, T.H., Fidock, D.A., Winzeler, E.A., Diagona, T.T., 2010. Spiroindolones, a potent compound class for the treatment of malaria. *Science* 329 (5996), 1175–1180. <https://doi.org/10.1126/science.1193225>.
- Shi, F., Waldo, J.P., Chen, Y., Larock, R.C., 2008. Benzynes click chemistry: synthesis of benzotriazolones from benzynes and azides. *Org. Lett.* 10 (12), 2409–2412. <https://doi.org/10.1021/ol800675u>.
- Sonoiki, E., Ng, C.L., Lee, M.C.S., Guo, D., Zhang, Y.-K., Zhou, Y., Alley, M.R.K., Ahyong, V., Sanz, L.M., Lafuente-Monasterio, M.J., Dong, C., Schupp, P.G., Gut, J., Legac, J., Cooper, R.A., Gamo, F.-J., DeRisi, J., Freund, Y.R., Fidock, D.A., Rosenthal, P.J., 2017. A potent antimalarial benzoxaborole targets a *Plasmodium falciparum* cleavage and polyadenylation specificity factor homologue. *Nat. Commun.* 8, 14574 <https://doi.org/10.1038/ncomms14574>.
- Stec, J., Onajole, O.K., Lun, S., Guo, H., Merenbloom, B., Vistoli, G., Bishai, W.R., Kozikowski, A.P., 2016. Indole-2-carboxamide-based MmpL3 inhibitors show exceptional antitubercular activity in an animal model of tuberculosis infection. *J. Med. Chem.* 59 (13), 6232–6247. <https://doi.org/10.1021/acs.jmedchem.6b00415>.
- Tahlan, K., Wilson, R., Kastrinsky, D.B., Arora, K., Nair, V., Fischer, E., Barnes, S.W., Walker, J.R., Alland, D., Barry 3rd, C.E., Boshoff, H.I., 2012. SQ109 targets MmpL3, a membrane transporter of trehalose monomycolate involved in mycolic acid donation to the cell wall core of *Mycobacterium tuberculosis*. *Antimicrob. Agents Chemother.* 56 (4), 1797–1809. <https://doi.org/10.1128/AAC.05708-11>.
- Tobin, C.M., Knoll, L.J., 2012. A patatin-like protein protects *Toxoplasma gondii* from degradation in a nitric oxide-dependent manner. *Infect. Immun.* 80 (1), 55–61. <https://doi.org/10.1128/IAI.05543-11>.
- Turner, R.J., Charlton, S.J., 2005. Assessing the minimum number of data points required for accurate IC₅₀ determination. *Assay Drug Dev. Technol.* 3 (5), 525–531. <https://doi.org/10.1089/adt.2005.3.525>.
- Van Voorhis, W.C., Adams, J.H., Adelfio, R., Ahyong, V., Akabas, M.H., Alano, P., Alday, A., Alemán Resto, Y., Alsibaee, A., Alzuale, A., Andrews, K.T., Avery, S.V., Avery, V.M., Ayong, L., Baker, M., Baker, S., Ben Mamoun, C., Bhatia, S., Bickle, Q., Bounaadja, L., Bowling, T., Bosch, J., Boucher, L.E., Boyom, F.F., Brea, J., Brennan, M., Burton, A., Caffrey, C.R., Camarda, G., Carrasquilla, M., Carter, D., Belen Cassera, M., Chih-Chien Cheng, K., Chindaoudomsate, W., Chubb, A., Colon, B. L., Colón-López, D.D., Corbett, Y., Crowther, G.J., Cowan, N., D'Alessandro, S., Le Dang, N., Delves, M., DeRisi, J.L., Du, A.Y., Duffy, S., Abd El-Salam El-Sayed, S., Ferdig, M.T., Fernández Robledo, J.A., Fidock, D.A., Florent, I., Fokou, P.V., Galstian, A., Gamo, F.J., Gokool, S., Gold, B., Golub, T., Goldgof, G.M., Guha, R., Guigumede, W.A., Gural, N., Guy, R.K., Hansen, M.A., Hanson, K.K., Hemphill, A., Hooft van Huijsduijn, R., Horii, T., Horrocks, P., Hughes, T.B., Huston, C., Igarashi, I., Ingram-Sieber, K., Itoe, M.A., Jadhav, A., Naranuntarat Jensen, A., Jensen, L.T., Jiang, R.H., Kaiser, A., Keiser, J., Ketat, T., Kicka, S., Kim, S., Kirk, K., Kumar, V.P., Kyle, D.E., Lafuente, M.J., Landfear, S., Lee, N., Lee, S., Lehane, A.M., Li, F., Little, D., Liu, L., Llinás, M., Loza, M.I., Lubar, A., Lucantoni, L., Lucet, I., Maes, L., Mancama, D., Mansour, N.R., March, S., McGowan, S., Medina Vera, I., Meister, S., Mercer, L., Mestres, J., Mfopa, A.N., Misra, R.N., Moon, S., Moore, J.P., Morais Rodrigues da Costa, F., Müller, J., Muriana, A., Nakazawa Hewitt, S., Nare, B., Nathan, C., Narradood, N., Nawaratna, S., Ojo, K.K., Ortiz, D., Panic, G.,

- Papadatos, G., Parapini, S., Patra, K., Pham, N., Prats, S., Plouffe, D.M., Poulsen, S. A., Pradhan, A., Quevedo, C., Quinn, R.J., Rice, C.A., Abdo Rizk, M., Ruecker, A., St Onge, R., Salgado Ferreira, R., Samra, J., Robinett, N.G., Schlecht, U., Schmitt, M., Silva Villela, F., Silvestrini, F., Sinden, R., Smith, D.A., Soldati, T., Spitzmüller, A., Stamm, S.M., Sullivan, D.J., Sullivan, W., Suresh, S., Suzuki, B.M., Suzuki, Y., Swamidass, S.J., Taramelli, D., Tchokouaha, L.R., Theron, A., Thomas, D., Tonissen, K.F., Townson, S., Tripathi, A.K., Trofimov, V., Udenze, K.O., Ullah, I., Vallières, C., Vigil, E., Vinetz, J.M., Voong Vinh, P., Vu, H., Watanabe, N.A., Weatherby, K., White, P.M., Wilks, A.F., Winzeler, E.A., Wojcik, E., Wree, M., Wu, W., Yokoyama, N., Zollo, P.H., Abla, N., Blasco, B., Burrows, J., Laleu, B., Leroy, D., Spangenberg, T., Wells, T., Willis, P.A., 2016. Open source drug discovery with the malaria box compound collection for neglected diseases and beyond. *PLoS Pathog.* 12 (7), e1005763 <https://doi.org/10.1371/journal.ppat.1005763>.
- Veber, D.F., Johnson, S.R., Cheng, H.Y., Smith, B.R., Ward, K.W., Kopple, K.D., 2002. Molecular properties that influence the oral bioavailability of drug candidates. *J. Med. Chem.* 45 (12), 2615–2623. <https://doi.org/10.1021/jm020017n>.
- Welsch, M.E., Snyder, S.A., Stockwell, B.R., 2010. Privileged scaffolds for library design and drug discovery. *Curr. Opin. Chem. Biol.* 14 (3), 347–361. <https://doi.org/10.1016/j.cbpa.2010.02.018>.
- Wilcken, R., Zimmermann, M.O., Lange, A., Joerger, A.C., Boeckler, F.M., 2013. Principles and applications of halogen bonding in medicinal chemistry and chemical biology. *J. Med. Chem.* 56 (4), 1363–1388. <https://doi.org/10.1021/jm3012068>.
- Witola, W.H., Zhang, X., Kim, C.Y., 2017. Targeted gene knockdown validates the essential role of lactate dehydrogenase in *Cryptosporidium parvum*. *Int. J. Parasitol.* 47 (13), 867–874. <https://doi.org/10.1016/j.ijpara.2017.05.002>.
- Woolsey, I.D., Valente, A.H., Williams, A.R., Thamsborg, S.M., Simonsen, H.T., Enemark, H.L., 2019. Anti-protozoal activity of extracts from chicory (*Cichorium intybus*) against *Cryptosporidium parvum* in cell culture. *Sci. Rep.* 9 (1), 20414. <https://doi.org/10.1038/s41598-019-56619-0>.
- Wu, R.Z., Zhou, H.Y., Song, J.F., Xia, Q.H., Hu, W., Mou, X.D., Li, X., 2021. Chemotherapeutics for *Toxoplasma gondii*: molecular biotargets, binding modes, and structure-activity relationship investigations. *J. Med. Chem.* 64 (24), 17627–17655. <https://doi.org/10.1021/acs.jmedchem.1c01569>.
- Zhang, Y.-K., Plattner, J.J., Easom, E.E., Jacobs, R.T., Guo, D., Freund, Y.R., Berry, P., Ciaravino, V., Erve, J.C.L., Rosenthal, P.J., Campo, B., Gamo, F.-J., Sanz, L.M., Cao, J., 2017. Benzoxaborole antimalarial agents. Part 5. Lead optimization of novel amide pyrazinyloxy benzoxaboroles and identification of a preclinical candidate. *J. Med. Chem.* 60 (13), 5889–5908. <https://doi.org/10.1021/acs.jmedchem.7b00621>.
- Zhou, C.-H., Wang, Y., 2012. Recent researches in triazole compounds as medicinal drugs. *Curr. Med. Chem.* 19 (2), 239–280. <https://doi.org/10.2174/092986712803414213>.
- Zhou, Y., Fomovska, A., Muench, S., Lai, B.-S., Mui, E., McLeod, R., 2014. Spiroindolone that inhibits PfATPase4 is a potent, cidal inhibitor of *Toxoplasma gondii* tachyzoites *in vitro* and *in vivo*. *Antimicrob. Agents Chemother.* 58 (3), 1789–1792. <https://doi.org/10.1128/AAC.02225-13>.